Expression of Interest

REDTOP: Rare Eta Decays with a TPC for Optical Photons

Y. Alexahin, A. Pla-Dalmau, J. Dey, V. Di Benedetto, E. Gianfelice-Wendt, E. Hahn, D. Jensen, C. Johnstone, J. Johnstone, J. Kilmer, G. Krnjaic, T. Kobilarcik, A. Kronfeld, K. Krempetz, M. May, A. Mazzacane, N. Mokhov, W. Pellico, V. Pronskikh, E. Ramberg, J. Rauch, L. Ristori, G. Sellberg, G. Tassotto

Fermi National Accelerator Laboratory

J. Comfort, P. Mauskopf, D. McFarland, L. Thomas

Arizona State University

I. Pedraza, D. Leon, S. Escobar, D. Herrera, D Silverio

Benemerita Universidad Autonoma de Puebla

A. Alqahtani

Brown University, Providence, Rhode Island

F. Ignatov

Budker Institute of Nuclear Physics – Novosibirsk

P. Sanchez-Puertas

Institute of Particle and Nuclear Physics – Charles University Prague

C. Gatto*

Istituto Nazionale di Fisica Nucleare – Sezione di Napoli and Northern Illinois University

W. Baldini

Istituto Nazionale di Fisica Nucleare – Sezione di Ferrara

R. Carosi, A. Kievsky, M. Viviani

Istituto Nazionale di Fisica Nucleare – Sezione di Pisa

W. Krzemień, M. Silarski, M. Zielinski

Institute of Physics, Jagiellonian University, 30-348 Krakow

S. Pastore

Los Alamos National Laboratory

M. Berlowski

National Centre for Nuclear Research – Warsaw

G. Blazey, M. Syphers, V. Zutshi, P. Chintalapati

Northern Illinois University

M. Pospelov

Perimeter Institute for Theoretical Physics, Waterloo

Y. Kahn

Princeton University, Princeton

A. Gutierrez, B. Fabela, M. A. Hernadez-Ruiz

Universidad Autonoma de Zacatecas

L. E. Marcucci

Universita' di Pisa and INFN

C. Siligardi, S. Barbi, C. Mugoni

Universita' di Modena e Reggio Emilia

M. Guida

Universita' di Salerno and INFN – Sezione di Napoli

J. Konigsberg

University of Florida

S. Gardner, J. Shi, X. Yan

University of Kentucky

R. Rusack

University of Minnesota

A. Kupsc

University of Uppsala

(The REDTOP Collaboration)[†]

[*] Email gatto@fnal.gov

[†] Homepage: http://redtop.fnal.gov

EXECUTIVE SUMMARY

This Expression of Interest is submitted as a request for a clear endorsement of the physics goals and the continued development towards full approval for running the REDTOP experiment at Fermilab. The endorsement will support a pending R&D proposal to DOE by members of the Collaboration as well as requests for base research funding at several funding agencies.

The REDTOP project has two preeminent goals. First, it aims to improve the sensitivity level of key physics conservation laws by several orders of magnitude beyond those of previous experiments. In doing so, it will open doorways for possible Physics Beyond the Standard Model including dark matter and energy, and/or new forces.

Second, to meet the challenge, REDTOP will extend and develop new and innovative detector technology. Precision timing capabilities will be implemented for the dual-readout calorimeter design from the T1015 (ADRIANO) project at Fermilab. The features will provide many new opportunities for future experiments in Particle and Nuclear Physics, and possibly other fields as well.

The REDTOP measurements will focus on decays of the η and η' mesons produced by protons beams of a few GeV energy. Extensions to kaon and muon beams will also be possible. Early measurements will be aimed at testing C, CP, and T conservation laws to many orders of magnitude below current levels.

Dedicated attention will be given to four “Golden Channels" of great interest:

- Certain definitive asymmetries that might be found in the Dalitz plot of the decay $\eta \to \pi^+\pi^-\pi^0$ would be evidence of C and/or CP violation. Existing data are far from definitive, and a REDTOP-sized sample will be needed.

- The decay $\eta \to \gamma A'$, with $A' \to e^+e^-$ or $\mu^+\mu^-$, provides two opportunities for new physics. They include vector dark photons A' from e^+e^- pairs, such as a possible one near 17 MeV. In addition, searches for scalar e^+e^- pairs could support a postulated light gauge boson as a mediator of a fifth, milli-weak force.

- The decay $\eta \to \pi^0 H$, where $H \to e^+e^-$, is a Higgs-like scalar. A 2-photon intermediate state ($\eta \to \pi^0\gamma\gamma$) conserves C, while a 1-photon mechanism ($\eta \to \pi^0\gamma \to \pi^0 e^+e^-$) violates C. Significant enhancement of the branching ratio above 2-photon models will indicate both C violation and the presence of two mechanisms.

REDTOP has a collection of simulation codes that are specially adapted to the needs of the project. Simulations of aspects of the experiment have shown the necessity for a more advanced calorimeter, and will help to guide its design. Preliminary simulations of some of the “Golden Channels" decays indicate that the sensitivity and resolution goals of REDTOP are likely to be reached.

The REDTOP detector has three advanced and novel components that must work together. They include an Optical TPC, a dual-readout calorimeter with high granularity and precision timing, and an Active Muon Polarimeter (which may or may not need separate apparatus).

A funding proposal has been submitted to DOE for support to extend the ADRIANO design to a new ADRIANO2 calorimeter that will have the additional and necessary granularity and precision timing features.

Beam from the Fermilab Delivery Ring at 8 GeV will need to be decelerated to 2-3 GeV for REDTOP. Designs of the necessary modifications, with minimal interference to other projects, are well underway.

The beam will be delivered to the AP50 enclosure of the Delivery ring. The door to AP50 is too small for the full detector system to be moved in altogether. Plans for modifying the detector and procedures for moving it are underway.

Although it appears that there are no significant radiation shielding concerns, calculations of effects from the intense beam and its halo on the target assembly raise some concerns about potential radiation damage and detector aging. Studies are continuing and several possible mitigations are being identified.

An initial design of a trigger system has been made. The raw signal rate will be quite large, but overall manageable. REDTOP will be a good opportunity to test and develop Particle Flow Algorithms for removing large backgrounds.

I. INTRODUCTION

It is now generally accepted that the Standard Model (SM) is not a complete description of nature. The exact nature of dark energy, dark matter, neutrino mass, and the baryon asymmetry of the universe (BAU) are among the very interesting questions that must find answers beyond the framework of the SM. These and similar issues provide strong hints that physics Beyond the Standard Model (BSM) could contain new particles and/or forces that may violate some of the discrete symmetries of the universe. Conservation laws with their underlying symmetry principles are at the heart of physics, from translation invariance in space-time leading to conservation of momentum and energy, to the symmetries and additive quantum numbers of modern particle physics. Symmetry violation is also important: the baryon asymmetry, for example, can arise only with violations of charge conjugation, the combined CP, and baryon number.

The REDTOP experiment is primarily intended to look for new violations of these basic symmetries, motivated by our current understanding that the violations within the SM do not suffice to generate the observed BAU. Our main focus will be on very rare decays of the η and η' mesons. The additive quantum numbers for these particles are all zero, the same as for the vacuum, with the exception of their negative parity, leading to the suppression of SM decays. An attractive feature of the η meson is that it is flavor neutral, so its SM C- and CP-violating interactions are known to be very small. Thus, rare η decays are a promising place to look for BSM effects. From the Standard Model and various BSMs, such decays can provide distinct insights into the limits of conservation laws, and open unique doors to new ones at branching ratio sensitivity levels typically below 10^{-9}. Notably, however, current experimental upper limits for η decays are many orders of magnitude larger, so η decays have not been competitive with rare decays of flavored mesons. The sensitivity goal of REDTOP is better than 10^{-11} for most decay modes, based on an estimated yield of more than 10^{13} η mesons per year. Production cross sections for the η' are about 1/100 those for the η. Numerous and unprecedented opportunities for constraining new physics will thus become available.

II. PHYSICS MEASUREMENTS

We have compiled an extensive list of possible measurements that can be made with REDTOP. They can be grouped into 6 categories, as outlined in Appendix A. Although the scope of the experiment is large, we shall showcase here only a few of the most interesting and potentially influential ones, presenting those with both a high degree of physics interest and real practical prospects for a meaningful result.

Typical final states in REDTOP consist of a neutral particle (pion or photon) and two charged particles (pions or leptons). Asymmetries in the Dalitz plot of $\eta \to \pi^+\pi^-\pi^0$ are sensitive to CP violation. The l^+l^- final state could, as conjectured by several BSMs, come from an intermediate particle, such as a dark photon or a light Higgs-like scalar boson. To distinguish these events from the SM background such as $\eta \to \gamma l\bar{l}$ (BR $\sim 10^{-3}$), and other backgrounds from the combinatorics in π^0 reconstruction, pion-lepton misidentification, photon conversion, and from the baryons generated by the nuclear scattering of the beam, a new and innovative detector is being designed.

II.A. C, T, and CP VIOLATION

The light pseudoscalar mesons π^0, η, and η' have very special roles for exploring and testing conservation laws. The π^0 has a long history of such tests and has established tight upper limits of

charge (C) and lepton flavor (LF) violations [PDG]. All of the additive quantum numbers for the η and η' are zero, and they differ from those of the vacuum by their parity. Due to the opposite G parities of the π^0 and $\eta^{(\prime)}$, couplings via strong interactions are suppressed. Thus, tests of C and CP in electromagnetic interactions are much more directly accessible in η and η' decays, limited mainly by the flux of such mesons [Nef94]. In addition, such decays can provide tests of P, T, CT, PT, and even CPT.

Almost all searches for symmetry violations in $\eta^{(\prime)}$ decays are upper limits in the range of 10^{-5} or higher [PDG]. An exception is the decay $\eta \to 4\pi^0$ at $< 6.9 \times 10^{-7}$, based on a sample of 3×10^7 η mesons [Prak00]. Most models of symmetry violations for various decay processes are at or below the level of 10^{-9}, often by several orders of magnitude. As discussed in Sec. II.C, no other planned $\eta^{(\prime)}$ experiment expects an event yield capable of reaching the sensitivity needed to probe branching ratios at the 10^{-9} level.

II.A.1. $\pi^+\pi^-\pi^0$ Dalitz Asymmetries

The decay $\eta \to \pi^+\pi^-\pi^0$ has a large decay branching fraction (22.7%). It violates G parity, but can occur because isospin symmetry is broken by the non-zero up-down quark mass difference. Recent data exist for this process [Amb08, WASA14, KLOE-CP]. A Dalitz plot can be made in terms of the two variables

$$X = \sqrt{3}\frac{T_+ - T_-}{Q} \qquad \text{and} \qquad Y = \frac{3T_0}{Q} - 1 \tag{1}$$

where the pion kinetic energies in the η rest frame are (T_+, T_-, T_0),and $Q = T_+ + T_- + T_0$ is the decay Q-value. The squared amplitude for the Dalitz distribution can be expressed as

$$|\mathcal{A}(X,Y)|^2 = \rho(X,Y) = N(1 + aY + bY^2 + cX + dX^2 + eXY + fY^3 + gX^2Y + hX^3) \tag{2}$$

where N is a normalization constant. With $m_{\pi^+} = m_{\pi^-}$, the distribution is expected to be symmetric about $X = 0$. Thus, non-zero coefficients for terms with odd powers of X (c, e, h) indicate C violation with no selection of isospin ΔI. Moreover, an analysis of the partial wave amplitudes contributing in the decay of a C-even, $J = 0$ meson state to $\pi^+\pi^-\pi^0$ reveals that terms of odd X in η decay are both C and CP odd [Gard04]. Other asymmetries between quadrants or sextants in the distribution can test C violation with $\Delta I = 1$ or 2 [Lay72].

Analysis of the data accumulated to date is complex, and results for the asymmetries have substantial uncertainties. Recent results for the C-violating parameters are [WASA14] are

$$c = -0.007 \pm 0.009(\text{stat}), \tag{3}$$

$$e = -0.020 \pm 0.023(\text{stat}) \pm 0.029(\text{syst}). \tag{4}$$

For a, b, d, and f, the differences in the values between two recent experiments [Amb08, WASA14] are between 0.6 and 2.5 standard deviations. Any definitive asymmetries would be evidence of C and CP violation. REDTOP can vastly improve the accuracy of the measurements and resolve the discrepancies. Including estimates of trigger efficiency and a reconstruction efficiency of 1%, we expect to achieve an analyzed sample of 10^9 events.

II.A.2. $\eta \to \pi^+\pi^- l^+ l^-$, $l = e, \mu$

In principle one could investigate CP violation by looking at E1 transitions of the photon in the decay $\eta \to \pi^+\pi^-\gamma$. A measurement of photon polarization would be required. Currently, a polarimeter is considered an option in the REDTOP apparatus. Another possible way to probe CP violation is when the photon is virtual and decays into a e^+e^- pair. CP invariance requires that in the asymmetry

$$A_\Phi = \frac{N[\sin(\Phi)\,\cos(\Phi) > 0] - N[\sin(\Phi)\,\cos(\Phi) < 0]}{N[\sin(\Phi)\,\cos(\Phi) > 0] + N[\sin(\Phi)\,\cos(\Phi) < 0]} \tag{5}$$

vanishes, where Φ is the angle between the decay planes of the electron-positron pair and the pions.

Measurements of such asymmetry have been made by the KLOE and WASA collaborations [Amb09, Adlarson]. The more recent WASA result is consistent with zero within the measurement errors. However, the statistical error, based on the production of $\sim 10^9$ η mesons largely dominates the measurement. The larger yields from REDTOP will improve the statistical error by almost two orders of magnitude; an improvement on the systematic error is under investigation. The two effects would bring the sensitivity level to a point where CP violation could be observed.

II.B. New Particles and Forces

II.B.1. $\eta \to \gamma e^+ e^-$

This process has a relatively large branching ratio corresponding to $\sim 7 \times 10^{-3}$ [PDG]. Consequently, REDTOP expects to detect a number of such final states in excess of 10^8, for a search of new particles decaying into a two-lepton final state, with the dark photon A' being an obvious candidate. Other experiments include: the HPS at JLAB [HPS] and PADME at Laboratori Nazionali di Frascati [PADME]. REDTOP, will do similar searches with hadron-produced eta mesons and, consequently, with very different statistical and systematic uncertainties.

Besides dark photons, eta decays are sensitive to other exotic particles. Thus, for example, a light baryonic charge force carrier B can be produced via $\eta \to \gamma B$ with subsequent decay of B into $\pi^0\gamma$, 3π or e^+e^- (depending on the mass of B).

Another exotic vector particle accessible with REDTOP is a light gauge boson, mediator of a fifth, milli-weak force. In recent years, several models have postulated the existence of such particles, in an attempt to reconcile anomalies found in experimental observations. In particular, secluded models of WIMP dark matter, characterized by a weak-scale rate for annihilation into light MeV-scale mediators have been proposed [Pospelov08] to explain the excess of positrons observed by PAMELA, ATIC, and the WMAP. Such mediators are metastable and decay into Standard Model states to which REDTOP is sensitive.

An interesting model with such a boson proposes to explain a 6.8σ anomaly in the invariant mass distributions of e^+e^- pairs produced in ^{8}Be nuclear transitions [Feng16]. The mass of such a gauge boson is estimated to be about 17 MeV. It is below the sensitivity of WASA, but accessible to REDTOP thanks to the boost imparted to the η meson in the lab frame. A plot of the regions already excluded for the $A' \to e^+e^-$ decay is shown in Fig. 1. There is plenty of discovery potential available to REDTOP.

The same fifth force would be able to reconcile the 3.6σ discrepancy between the predicted and

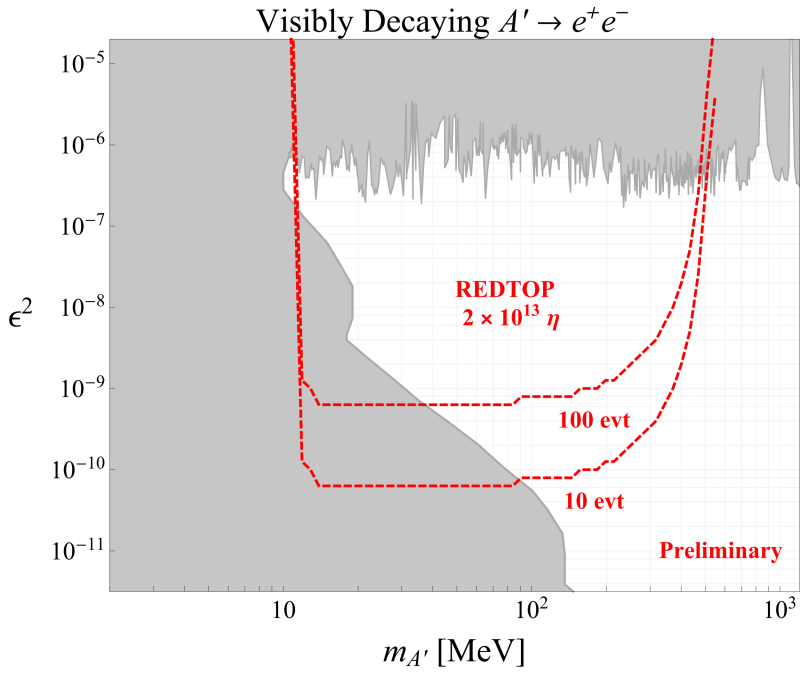

Figure 1. The shaded regions are excluded for the decay $A' \to e^+e^-$, leaving lots of room for REDTOP.

measured values of the muon's anomalous magnetic moment. In this respect, REDTOP is a nice complement to the Muon g-2 experiment E989 at Fermilab [G-2].

II.B.2. $\eta \to \pi^0\mu^+\mu^-$

The mechanism for the $\eta \to \pi^0\mu^+\mu^-$ (or e^+e^-) decay is usually described via a 2-photon intermediate state to conserve C: $\eta \to \pi^0\gamma\gamma$ along with $\gamma\gamma \to \mu\bar{\mu}$ via a triangle diagram. Branching ratios are calculated to be of the order of 10^{-9} [NgP92, NgP93, JS02], which should be well within the sensitivity of REDTOP. In the case of C violation, a 1-photon mechanism ($\eta \to \pi^0\gamma$, with $\gamma \to \mu\bar{\mu}$) is also possible [NgP92, JS02]. A significant enhancement of the branching ratio above the 2-photon model can indicate C violation. Branching ratios of $\sim 5 \times 10^{-6}$ for $\eta \to \mu^+\mu^-$, and $\sim 1 \times 10^{-7}$ for $\eta' \to \mu^+\mu^-$ have been estimated [Pet10, MSP16].

II.C. Other $\eta^{(\prime)}$ Experiments

The Crystal Ball experiment at the Brookhaven AGS was able to provide a few times 10^7 η mesons. It was subsequently moved to MAMI, and a goal there is to achieve another order of magnitude in η yield. Other facilities include KLOE [KLOE-CP] (via $\phi(1020) \to \eta\gamma$), WASA at COSY, and GlueX at JLAB, all with an η yield of 10^8 or more. To reach the more exacting levels needed for symmetry violations, the usable η flux must be increased by several orders of magnitude. Common searches for violation of C parity involve η decays into neutral channels with π^0s and an odd number of photons in the final state. Because $C = +1$ for the η and $C = -1$ for photons, positive detection of such states is clear evidence of C violation.

In addition to their key intrinsic merit regarding electromagnetic conservation laws, studies of neutral η decays will be critical to the development of the detector and techniques used by REDTOP.

III. PROTON BEAM REQUIREMENTS

Achieving the full set of goals of the experiment will require production and processing of at least 10^{13} η meson decays. The goals can be met by having a flux of 10^{11} protons per second on target, and a duty factor of over 75%. The Fermilab Booster routinely delivers 4×10^{12} protons per cycle at up to 15-Hz repetition rate. Thus, there should be an abundance of protons to meet the REDTOP goals. However, the Booster extraction kinetic energy is 8 GeV, well above the ∼2 GeV and 3 GeV needed for REDTOP to produce, respectively, η and η' mesons. A deceleration stage will be implemented.

III.A. Delivery System

The REDTOP program requires a proton flux of 10^{11} p/s with high duty factor ($> 75\%$) at a particle kinetic energy of 2-3 GeV. The Fermilab Booster can deliver 4×10^{12} protons every 15-Hz pulse and so can easily meet the overall rate. However, the output of the Booster is 8 GeV and the various accelerator systems connected to it operate at this energy or higher. Extracting beam from the Booster at energies lower than 8 GeV is feasible in principle but would require new extraction lines, civil construction, and long shutdown periods to the Fermilab program. A better approach is to deliver a 8-GeV beam from the Booster to the newly-commissioned Delivery Ring (previously the antiproton Debuncher Ring) and decelerate it to the desired final energy.

The beam scenario for REDTOP is envisioned as follows. Just as is to be done for the Muon g-2 and for the Mu2e experiments, a single 15-Hz pulse from the Booster would be extracted to the Recycler Ring in the Main Injector tunnel and re-bunched into four bunches of 10^{12} protons each with 2.4 MHz spacing. These four bunches would be transferred to the Delivery Ring (DR) and captured by using the same 2.4-MHz system to be employed by Mu2e. (Note: Mu2e accepts one bunch at a time, but all four would be transferred simultaneously for REDTOP.) The 2.4-MHz RF system will be used to decelerated the beam from 8 GeV to 2 GeV over a period of approximately 5 seconds. Then, by using the slow resonant extraction system that is being installed for Mu2e, the beam will be slow-spilled toward the REDTOP experiment over a period of about 40 seconds. After the spill, the magnets are ramped back to their 8-GeV level in about 5 seconds and the process repeated. Thus, the duty factor will be approximately 80% and the particle spill rate during extraction will be approximately the desired rate of $4 \times 10^{12}/40 = 10^{11}$/sec. The REDTOP Booster pulses would come from the spare 15-Hz pulses as in the Muon g-2 and Mu2e programs and thus have no impact on the neutrino program timeline. Fig. 2 shows a schematic of the Muon Campus complex.

For Muon g-2 as well as for Mu2e, the Delivery Ring will be operated DC. The muon momentum for Muon g-2 operations is approximately 3.1 GeV/c, not far from the REDTOP desired momentum (2.8 GeV/c for 2 GeV kinetic energy). The beam delivery system for Muon g-2 has already had a commissioning run that has verified the large phase space admittance of the system for the muon beam; it is much larger than will be required for proton operations. Alterations to the DR power supply systems and to the RF system will be required, however, in order to perform the beam deceleration. An initial look at the magnet and RF requirements for the DR to perform the above manipulations for REDTOP suggests that a reconfiguration of the power supply system is needed to ramp the magnets down and up in a suitable amount of time. The inductance of the magnet system generates a natural time constant of approximately 7 s. If inverting power supply components were to be installed, a ramp time of ∼5 s is likely achievable.

For deceleration, the existing 2.4 MHz cavity being installed in the DR for Mu2e would not be

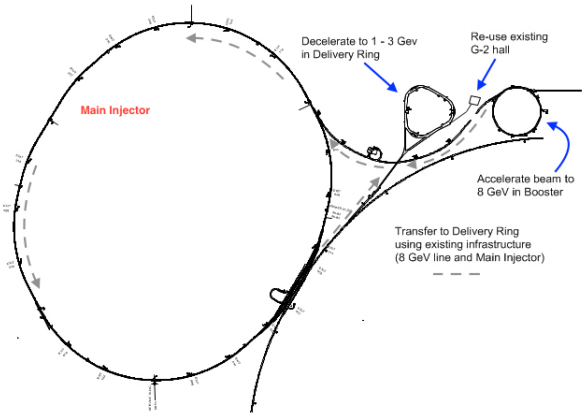

Figure 2. The Fermilab accelerator complex for REDTOP operation.

sufficient for REDTOP, mainly due to the inherent frequency shift that would occur in going from 8 GeV to 2 GeV kinetic energy. However, if a second RF cavity of the same kind were installed, but tuned to a slightly lower frequency, the combination of the two could be used for the required deceleration. A third cavity would provide even more latitude in the operation, but may not be necessary. A spare cavity has already been produced for Mu2e and could be utilized in this capacity. These two cavities are identical to those produced for the Recycler RF upgrade and hence the acquisition of a third cavity, should that be deemed desirable, would be straightforward. In addition to upgrades to the main power supply system and the additional cavity, the ring would need to be upgraded to a ramped correction magnet system, primarily in the form of time-dependent power supply controls.

During early discussions of this scenario it was realized that the beam would be required to pass through the "transition energy" of the DR during deceleration. This particular energy – where the revolution frequency is independent of small deviations in momentum – requires particular care to avoid beam losses and occurs at approximately 6 GeV in the current DR configuration. However, a solution has been found whereby the focusing characteristics of the DR can be altered to push this transition energy up above 8 GeV [Johnstone]. Hence, crossing the transition can be avoided altogether. The solution involves no new magnetic elements, but rather straightforward adjustments to the powering of existing elements which will require either new cabling and new power supplies or the implementation of new current shunts on some of the magnets, similar to what is already used in the DR system in many locations. The lattice functions are kept constant throughout the straight sections in which beam is injected and extracted, whereas the dispersion function through the bending regions, which determines the transition energy, is altered appropriately. (See Fig. 3.) Though the beam size (which varies with the square root of the functon β in this figure) is approximately doubled in some locations, it is still well contained within the DR aperture. Once the beam is decelerated to below 6 GeV, the optics configuration can be programmed back to its original form before extraction takes place if this is deemed necessary.

A second early concern with the scenario was regarding the use of the slow resonant extraction hardware at the lower extraction energies. Recent analytical calculations and computer simulations of the slow spill process at 1.9 GeV have shown that the DR apertures and hardware being developed for Mu2e will be sufficient for use at 1.9 GeV, and hence for intermediate energies as well. Assuming that REDTOP would not run parasitically with Mu2e, the electrostatic septum used during slow spill can be moved radially by 8 mm to generate the appropriate "step size" of the particles jumping

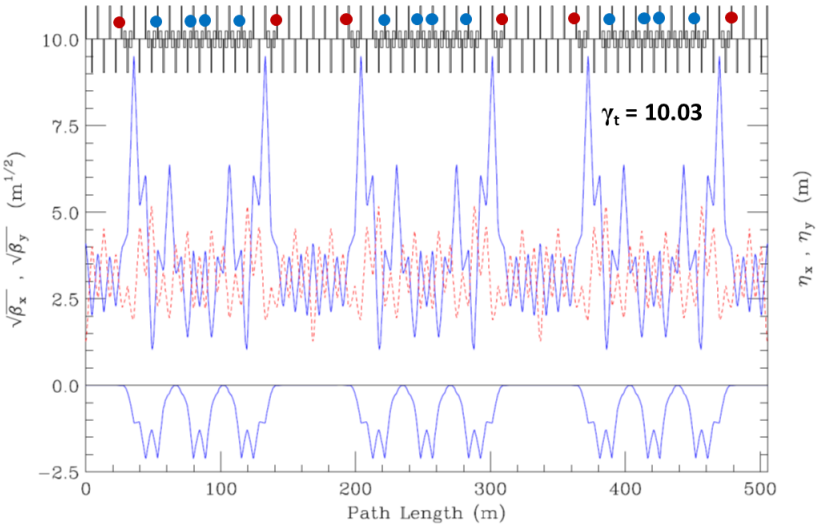

Figure 3. Lattice functions of the Delivery Ring with new, high-transition optics producing $\gamma_t = 10.5$.

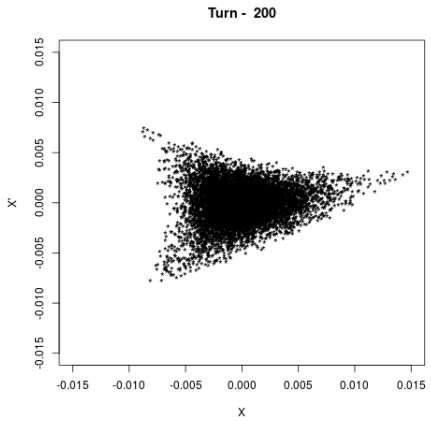

Figure 4. Result of a preliminary particle tracking simulation showing the horizontal transverse phase space created by the slow resonant-extraction system. Here, the particle displacement x is in meters, its slope x' in radians. The orientation of the triangular region can be rotated by the sextupole magnet system. Ultimately particles are "spilled" out of the distribution at the tips of the triangular phase space, whereby they jump across an electrostatic wire septum and into the extraction channel toward the REDTOP experiment.

across the wire septum during the extraction process. This adjustment maintains a non-linear step size appropriate for a 1-1.5% extraction inefficiency. It is similar to that for Mu2e operations (it is actually more efficient at the lower energies) and the circulating beam will still have a full aperture of as much as 75 mm, well within the good field regions of the DR magnetic elements. It should be pointed out again that the rates being requested of REDTOP are far below the rates for Mu2e – 4×10^{12} every 50 seconds compared to 16×10^{12} every 1.3 seconds. An example phase space diagram employing REDTOP 2-GeV parameters is shown in Fig. 4.

Also relevant to the slow spill operation is the beam tube vacuum. For Mu2e the extraction process happens over a fraction of a second, whereas for REDTOP the process would take 40 seconds.

Beam-gas scattering, which would be a source of emittance growth and potential beam loss, will be a larger effect at lower beam momenta. For an average vacuum of 0.1 μtorr, typical of the DR system, the emittance growth rate at 2 GeV should be less than 0.1 π mm-mr/s which should be tolerable for the slow spill process. An engineering inspection of the ring has shown that there is plenty of space in the system to implement more pumping; further detailed studies will deem whether or not this option will be necessary.

Finally, the current plan is to install the REDTOP detector at the AP50 location on the antiproton ring. The DR tunnel has an experimental area that was used for the antiproton experiment E760 and associated counting room and lab space directly upstairs connected to the AP50 service building. The large service door-way to AP50 is a few inches shorter than the height of the experiment's calorimeter and so various solutions are being considered to handle installation. The tunnel in this straight-section location is quite wide and should be able to handle the manipulations required to steer the 2 GeV extracted beam into the experimental hall. Beam line optics design for the extracted beam transport system will begin in the upcoming months.

III.B. Radiation Shielding and Safety

The experimental hall proposed for REDTOP, AP50, is part of Fermilab's "Muon Campus" where two experiments are or will be running (Muon g-2 and Mu2e). All areas related to the Muon Campus are under close scrutiny by the Fermilab Safety Dept., and a full radiation shielding assessment has been recently completed and approved by the ESHQ Office. According to the latter, a maximum beam intensity of 3.60×10^{13} protons/hr at 8 GeV can be circulated and delivered in the accelerator complex where AP50 is located, with the current radiation shielding, while 2.20x10^{16} protons/hr canbe circulated with the modification foreseen for Mu2e. The latter rate corresponds to a maximum beam power circulated and dumped of 8 kW, to be compared with the 30 W proposed to run REDTOP as an η-factory, and the 50 W proposed for a later run as an η'-factory. In both cases, the proposed beam intensity is considerably smaller than the maximum allowed and it requires no refurbishing of the existing radiation shielding.

III.C. Radiation Damage and Detector Aging

The intense proton beam required for reaching REDTOP's physics goal is also expected to generate a radiation halo that will age and could potentially damage the detector. Descriptions of the detector components are contained in Sec. IV.

An analysis of the radiation flux expected throughout the detector has been performed with the MARS15 code [MARS15] and a geometrical model that reflects our baseline detector layout, along with an aluminum-Borated Polyethylene-barite beam dump. The result of a study for a 30-W proton beam with 1.8-GeV energy impinging onto the beryllium target systems is shown in Fig. 5. The plot represents the so-called "*1-MeV equivalent neutron fluence*" (NEQF) dose, which is commonly used to estimate the damage inflicted by radiation to photo-sensors.

The areas of concern are the photo-sensors around the vessel of the OTPC and the area around the beam pipe that is planned to be instrumented with a scintillating fiber tracker (cf. Sec. VII.E). A more detailed radiation flux analysis of such areas is described in Appendix B. The maximum NEQF flux illuminating the photo-sensors is located on the forward endplate of the of OTPC and is expected to be about $6 \times 10^5/\text{cm}^2/\text{s}$ (or $6 \times 10^{12}/\text{cm}^2$ integrated over 1 year), as shown in Fig. 22. The rate for the barrel is, in average, a factor of 5-6 lower (cf. Fig. 23). The currently recognized

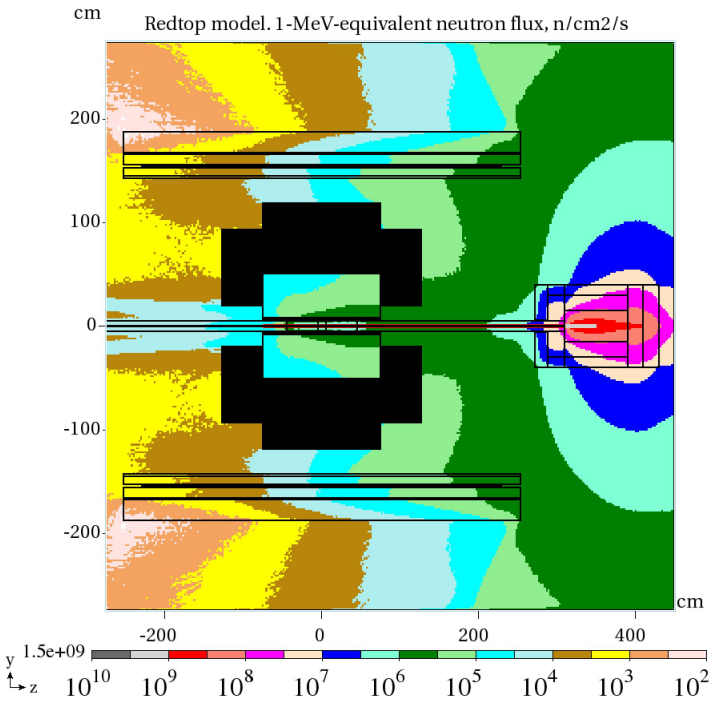

Figure 5. "*1-MeV equivalent neutron fluence*" dose expected in the REDTOP detector for a 30-W proton beam.

integrated limit for commercial SiPMs, the current baseline technology adopted for the OTPC, corresponds to about $10^{13}/\text{cm}^2$ NEQF. The value is uncomfortably close to the estimated flux in the end plates. A consequence is an increase in the dark count rate (DCR) of the sensors (typically, 50 kHz/mm^2 or 250 OTPC hits/evt for a 1-ns integration time). While the effect of such noise is expected to be minimal on the reconstruction of Čerenkov rings, a bigger issue would come from the saturation of the online systems which could compromise the data transfer of the compressed data from the detector to the L0 trigger systems. We are aware of the issue and plan to investigate it further. Possible roads we will consider to mitigate an increased DCR are:

- A larger bandwidth between the FEE and the L0 trigger systems;
- Cooling the SiPM's;
- Narrowing the integration time;
- Investigate new generation sensors (e.g. addition of trenches between pixels to reduce cross talk);
- Using Multichannel plates for the forward endplate and SiPMs for the remainder of the detector;
- Consider LAPPD instead of Sipm's, although the formers are not yet commercially available.

In addition to these items, the LHC Community is very active in this area and we expect to benefit greatly from the R&D performed by them.

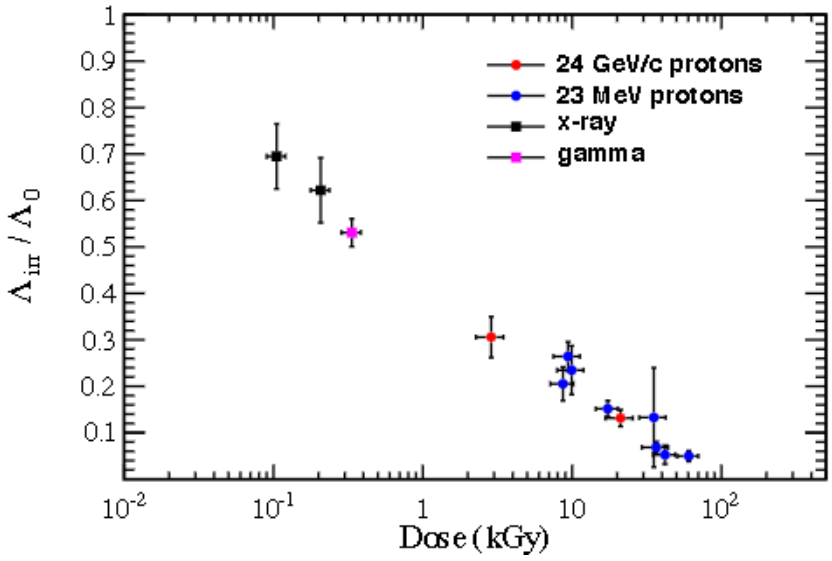

Figure 6. Change in attenuation length of a KURARAY SCSF-78 fiber ($\varnothing$250 μm) vs. integrated dose.

The area near the beam pipe, where the fiber tracker will be located, is currently unders study. A preliminary estimate of the integrated absorbed dose expected in that area is described in Appendix B. Recent studies by LHCb [Joram15] where fibers have been tested up to 60 kGy, is summarized in Fig. 6, where the change in attenuation length is plotted vs. the radiation dose. In the case of REDTOP, we expect that the fiber tracker would degrade considerably during a 1-year run, with the attenuation length of a typical KURARAY SCSF-78 fiber ($\varnothing$250 μm), diminishing from about 4 m to 10 cm. We are aware of the issues and plan to investigate them further.

III.D. AP50 Enclosure and Solenoid

REDTOP proposes to use the Finuda magnet [Bert99] from the Frascati Phi factory (DAPHNE). The Finuda magnet was built at Ansaldo. This magnet has the required field uniformity of better than 5% in the tracking volume. The magnet is superconducting with a total heat load of 22 Watts at 4.4 K and uses 0.4 gm/sec of liquefaction for the current leads. The radiation shield has a heat load of 100 Watts at 70 K. The magnet is cooled as a thermosiphon. A steel flux return yoke is also available.

The AP50 area was last used for E760 in the 1990s. E760 used liquid helium supplied by a CTI model 1400 liquefier which is still available and should easily handle the load of the Finuda magnet. A liquid nitrogen dewar will have to be moved to the location and a new source of compressed helium gas will be needed. E760 was supplied these products from the Tevatron cryogenic system which has been decommissioned.

The AP50 enclosure presents some mechanical challenges. Everything for the experiment must be installed through a drop hatch which is beside the enclosure. All the parts will fit down the hatch opening. The relationship of the hatch to the enclosure is shown in Fig. 7.

The Finuda magnet will fit down the hatch but must be rotated on its side 45 degrees to enter the enclosure from the hatch. Additionally, the opening from the hatch to the enclosure is too small

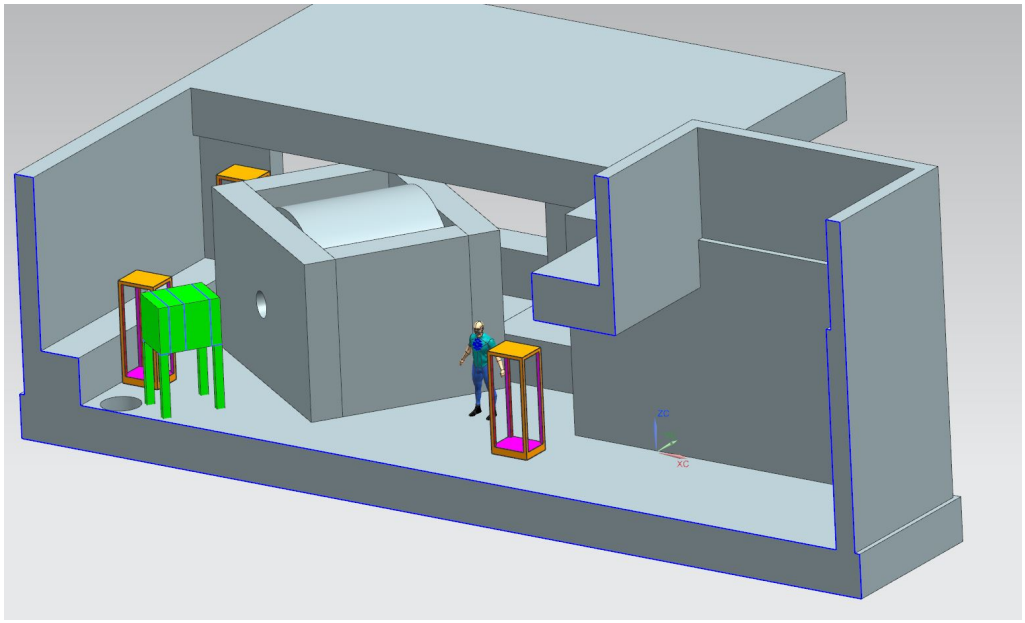

Figure 7. Layout of the AP50 enclosure.

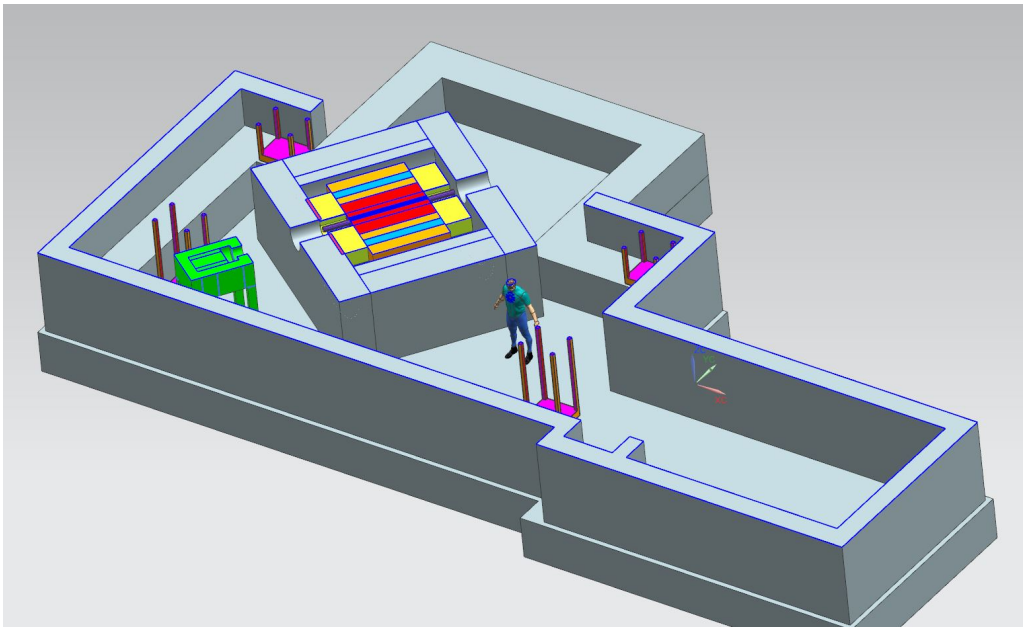

Figure 8. Yoke pieces of maximum size in the AP50 enclosure.

for the magnet and the lintel must be cut to allow the magnet to pass under. Facilities Engineering Services Section has been contacted and they agree that there are several methods that can be used to safely enlarge the opening for the magnet size.

The enclosure has only a small 2-ton jib crane that will not be useful for the REDTOP experiment. The original Finuda flux return steel will not fit in AP50, so a smaller size yoke is planned. Some very preliminary studies of magnet performance with a different yoke have been started.

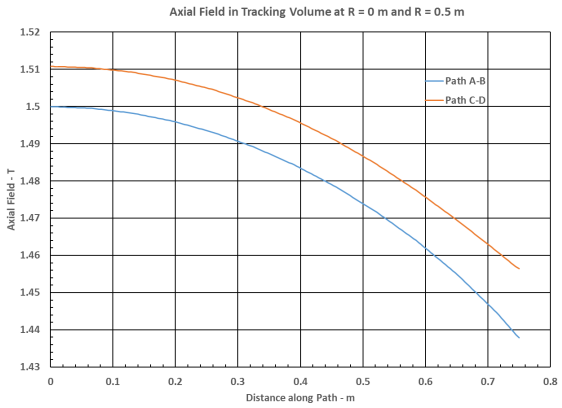

Figure 9. The solenoid field strength from the beamline to the solenoid yoke, for two different paths.

The maximum sizes of yoke pieces that can fit into the enclosure are shown in Fig. 8. An analysis of the magnet flux for the asymmetric yoke shown in Fig 7 is shown in Fig 9. The uniformity of the field is better than 4.1% over the entire tracking volume.

The size of the AP50 enclosure will limit the assembly of the experiment to be similar to that used for E760. Parts such as the yoke pieces will have to be assembled under the hatch and rolled into position on Hilman rollers in a specific order. The assembly order is as follows: (a) the upstream magnet yoke; (b) the beam right magnet yoke; (c) the magnet and detectors; (d) the downstream magnet yoke; and (e) the beam left magnet yoke. These yoke pieces may be assembled from smaller pieces of steel in the hatch area to avoid requiring a very large crane. Finally, the beam dump is moved in behind the detector. The detector elements will have to be mounted in the magnet bore in another building before the magnet is moved to the hatch and lowered. Additional engineering is required to determine if some elements of the detector can be repaired/replaced by just opening the yoke, or if the magnet must be removed from the enclosure.

IV. THE REDTOP DETECTOR

The detector contains several critical components that must work together to achieve the goals of the experiment. Three major components of the detector, the Optical TPC (OTPC), the ADRIANO2 calorimeter, and the active Muon Polarimeter, are novel technologies under active development. Thus, REDTOP will not only challenge fundamental physics limits, but also represents a step-up in detector technologies, paving the way for more challenging experiments in the future. In particular, we envisage that these technologies will be extended into the PIP-II era where events rates and pile-up are expected to be much higher than for REDTOP. A schematics of the detector is shown in Fig. 10. A description of its main components follows.

IV.A. The Target System

The target system (corresponding to the blue circles in Fig. 10) is composed by ten round foils of beryllium, each about 240 μm thick and about 1 cm in diameter. The target system is held in the center of a beryllium or carbon-fiber beam pipe by thin AlBeMet wires. The pipe will also help in maintaining a vacuum and in supporting an aerogel radiator attached to its external wall. A proton with 1.8 GeV of kinetic energy has a 0.5% probability to make an inelastic scattering in any of the

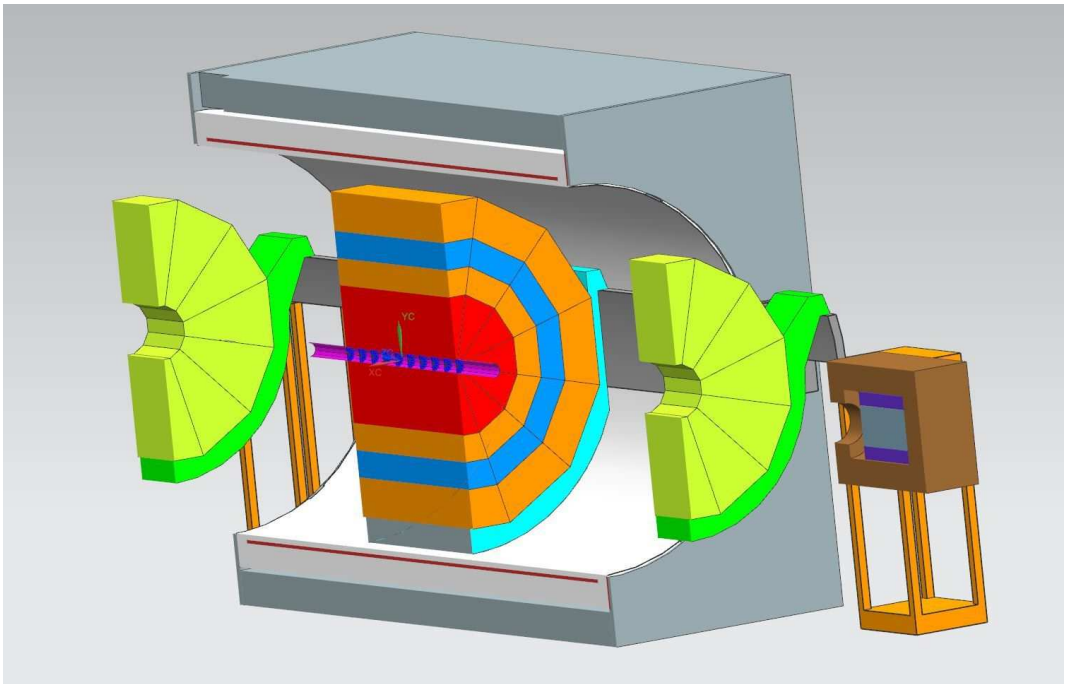

Figure 10. The REDTOP experimental apparatus.

foils. The probability that one such scattering would produce an η meson is about 0.4%. With an average beam intensity of the order of 1×10^{11} protons/sec, the number of η mesons produced in one year is expected to be about 2×10^{13}.

Differing from the use of a gaseous target (*e.g.* [WASA14]) the distributed targets will help to disentangle the η events backgrounds, the latter being mostly constituted by inelastically scattered protons from the target matter. The distance between foils is sufficient to identify the location of the primary vertex without ambiguities, while the tracking systems will provide $r\varphi$ coordinates. Finally, preliminary Monte Carlo simulations have indicated that the decay products of the η meson are minimally affected when traversing a very thin beryllium foil. The fraction of the beam absorbed by the target system is about 5%. Consequently, each beryllium foil will need to dissipate only 15 mW, easily achievable by thermal radiation and by conduction through the supporting metal wires.

IV.B. The Optical TPC

As with a conventional TPC, the OTPC (marked in red in Fig. 10) will measure the momentum and trajectory of a charged track through its deflection in a solenoidal magnetic field. However, rather than detecting the tracks via a ionization process in the gas, the Čerenkov effect is employed. The momentum of that particle is then reconstructed from the detection of the photons radiated from an aerogel layer along the inner radius of the OTPC, as well as from the gas, by using an array of photo-sensors mounted inside the outer radius of the OTPC. About 100,000 SiPMs are needed to cover the entire outer surfaces. The pattern of detected photons will also provide the position in space of the initial particle. The advantage of an OTPC over a conventional TPC is that it will be sensitive only to the fast particles (leptons and fast pions) entering the volume of the detector. In particular, hadrons and slower pions will be below the Čerenkov threshold and, therefore, will not be detected.

A prototype of an OTPC has been built and tested by the T1059 Collaboration at Fermilab [T1059]. The current design of the Čerenkov radiator is a 3-cm-thick aerogel shell supported by the beam pipe (the magenta ring in Fig. 10). Low-pressure nitrogen gas fills the remaining volume of the OTPC. The pressure is adjusted in order to have $n_D = 1.000145$. Muon particles with momenta larger than 160 MeV will radiate only in the aerogel. The radius, the center, and the skewness of the ring will help to determine their velocity. The e^+ and e^- will radiate in the aerogel as well as in the gas. The rings produced by such light particles have radii nearly independent of their velocities. They are also much larger than those for muons, which will aid in particle identification.

IV.C. The ADRIANO2 Calorimeter

Dual-readout calorimetry is a novel detector technique that has received considerable attention in the past few years. An implementation, named ADRIANO (A Dual-Readout Integrally Active Non-segmented Option), has been under development for several years at Fermilab [T1015-1, T1015-2, T1015-3]. It is based on the simultaneous measurements of the energy deposited by a hadronic or electromagnetic shower into two media with different properties. The first medium is usually a plastic scintillator. Consequently, any charged particle depositing energy in that medium will produce scintillation. The second medium is usually a heavy glass with high refractive index ($n_D \geq 1.8$) and high density ($\rho > 5.5$ g/cm^3). The latter medium will be sensitive only to charged particles above the Čerenkov threshold, which usually happens for the electromagnetic components of the shower (electrons and positrons or photons producing pairs). Furthermore, the high density of the medium will make it an ideal integrally active absorber for all particles impinging on the detector.

The rationale for employing such a calorimeter is that the large backgrounds from the vast majority of neutrons entering the detector can be easily rejected. Summing the Čerenkov (C) and the scintillation (S) signals will provide the total energy of the particle. Comparisons of the scintillation vs. the Čerenkov signals provides information about the ID of the particle that generated the shower. Furthermore, the different behavior in terms of S vs. C for muons and pions will complement the double aerogel systems for identifying the two species.

The calorimeter is indicated in orange in Fig. 10. Although the principle is good, Monte Carlo simulation studies carried out during the past year have clearly shown that the current ADRIANO design will not be adequate for REDTOP. Much better precision in energy resolution, precision timing, and particle identification are necessary. In the ADRIANO design, the energy signals are summed along the beam direction and do not provide reliable positions of the signals in that direction. To meet our goals, a proposal was recently submitted the the DOE Detector Research and Development program for the generic development of expanded capabilities that can be applied to many future experiments, with REDTOP as an example application. We will apply the new features to the design of an ADRIANO2 system. It will provide much finer granularity along the beam direction, timing precision to about 50 ps or better, and other benefits.

IV.D. The Active Muon Polarimeter

The Active Muon Polarimeter (the blue bars in Fig. 10) is an array of plastic scintillators and wire chambers inserted between the inner and the outer layers of the Calorimeter. They will detect the electrons and positrons emitted when a muon is stopped inside the Calorimeter, which occurs within a short range after the muon has lost all of its energy. The initial polarization of the muon is not lost in this process because the lead-glass used in ADRIANO2 is a homogeneous and isoscalar medium. If

the muon carries a non-null polarization, the electrons (or positrons) are emitted non-isotropically in the solenoidal magnetic field. The Active Muon Polarimeter will count those electrons; any unbalance in the left-right or front-backward counting is associated with a non-null transverse or longitudinal polarization of the initial muon. The current design of the Muon Polarimeter is based on the granular ADRIANO2 detector. It potentially could be able to measure the polarization of the muon. Further studies are required to establish the real need of a Muon Polarimeter in such configuration.

IV.E. The Solenoid

The REDTOP detector will be inserted inside a large superconducting solenoid (the white cylinder in Fig. 10) where a 0.6-T solenoidal field will be generated. The magnetic field will allow the OTPC to measure the transverse momentum of charged particles, and the Muon Polarimeter to measure the polarization of muons. The Finuda magnet [Bert99] from the Frascati Phi factory (DAPHNE) is being considered for that application.

IV.F. The Fiber Tracker

The initial baseline layout of REDTOP did not foresee the need for a tracker to determine the z position of tracks from an event. Our initial experience suggested that the pointing capabilities of the OTPC would be sufficient to reject the background from photon conversion in the aerogel and for establishing vertices. Further simulation studies (cf. Sec. VII) have indicated otherwise. A design of such tracker is still in progress and it proceeds in parallel with the physics and detector studies.

V. EVENT TRIGGER SYSTEM

The goal of producing 10^{13} etas per year, assuming 10^7 seconds of useful running time, translates to 10^6 etas per second which, in turn andgiven the eta production cross section, translates to 2×10^8 p-Be inelastic collisions per second. This rate can be achieved with a proton beam intensity of 10^{11} p/s and a Be target of 2×10^{-3} collision lengths ($\approx$ 1 mm thickness), possibly subdivided into a number of thinner layers.

The task of the REDTOP trigger is to reduce the event rate from the p-Be total inelastic collision rate of 2×10^8 Hz down to about 2×10^4 Hz of events to be permanently recorded. Assuming an average final event size of 10^4 bytes, this yield will produce an output data rate of 200 MB/s or about 2 PB/year, which we consider manageable.

The needed 10^4 reduction in event rate is achieved by two trigger stages, Level 0 (L0) and Level 1 (L1), each one resulting in a rate reduction of about 100. These two stages are preceded by a digitization and compression (DAC) stage. The DAC stage is directly attached to the front-end of the detector. Level 0 and Level 1 sit off the detector. A fiber optics network delivers data from the DAC to Level 0 and from Level 0 to Level 1. The events filtered by Level 1 are delivered to Level 2, a processor farm that performs event building, reconstruction, formatting and classification. A further rate reduction can possibly be achieved at Level 2, before permanent recording, if needed. Table I summarizes data and event rates into and out of the different stages.

Trigger stage	*Input event rate Hz*	*Event size bits*	*Input data rate bits/s*	*Event rejection*
Level 0	$2. \times 10^8$	1×10^4	2×10^{12}	100
Level 1	$2. \times 10^6$	$5. \times 10^4$	$1. \times 10^{11}$	100
Level 2	$2. \times 10^4$	$5. \times 10^4$	$1. \times 10^9$	1
Storage	$2. \times 10^4$	$1. \times 10^5$	$2. \times 10^9$	

Table I. Data and event rates for different stages

V.A. Digitize and Compress

The DAC hardware digitizes all data coming from the detector in real time, performs zero suppression, and data compression to reduce the amount of data to be transmitted to the following stages. No event selection is performed at this stage.

V.B. Level 0

The selection performed by Level 0 is based on simple global features of the events produced by p-Be inelastic collisions. Preliminary simulations suggest that, by setting thresholds on the occupancy of the OTPC and on the total energy deposited in the calorimeter, we can achieve the needed rejection factor of 100 while preserving a satisfactory efficiency on interesting physics processes.

The data rate into Level 0 is estimated from preliminary Monte Carlo simulations by observing that each p-Be collision produces an average of about 10 Kb of data, after zero suppression and compression by the DAC. At a collision rate of 200 MHz the data rate corresponds to 2 Tb/s. Such a data rate can be comfortably transmitted by a network of a few hundred optical fiber links. Because all data from the detector are continuously digitized in the front-end and immediately transmitted to the following stages, trigger latency is not a problem, at least to first order. Therefore the Level-0 logic can be heavily pipelined. Although a new event will arrive, on average, every 5 ns, the time taken to make a decision on a specific event can be much longer, possibly microseconds.

V.C. Level 1

Level-1 rejection will be based on the identification of a pair of leptons (electrons or muons).

A significant challenge of the REDTOP trigger will be to design specialized processors to achieve the needed rejection factor of order 100 by reconstructing Čerenkov rings from muons and electrons in the OTPC, discriminating photon conversions in the Čerenkov radiator and beam pipe with high efficiency, at an event rate of 2 MHz. We believe that this selectivity can only be achieved with specialized hardware, possibly based on massive use of FPGAs.

To gain more time to process each event, we can adopt a time multiplexing strategy. We anticipate that events will be distributed to a bank of identical processors in a round-robin fashion. The larger the number of processor, the more time each one of them will have to process one event. A time multiplexing of factor of 10 will allow each processor 5 microseconds, on average, to process each event, which seems adequate for the task.

As a comparison, a demonstrator of the Level-1 tracking trigger for CMS Phase II has recently shown that ten identical, FPGA-based, processors, housed in a single ATCA crate and operated in

a time-multiplexing mode, can process events coming at a rate of 40 MHz from a unit corresponding to 1/48 of the CMS tracker. Each unit contained the order of 500 hits and was carried by about 400 fibers. All the tracks with a P_t above 3 GeV/c could be reconstructed with high efficiency and a latency of a few microseconds. The rates processed and the complexity of the problem are on the same level as expected for REDTOP L1 trigger.

V.D. Level 2

The Level-2 processor farm will receive 20 kHz of events, equivalent to a data rate of 200 MB/s, from Level 1. These events need to be reconstructed and formatted for permanent storage. We assume that this task can be completed by using less than 100 ms of CPU time and that, consequently, a farm of 2000 CPUs should be adequate for the job.

This same processor farm can be used for "data production" when the experiment is not taking data. Additional information on our methods for estimating the data rates can be found in appendix C.

VI. PHYSICS AND DETECTOR STUDIES

Although REDTOP will make only modest demands on a beam (low energy, CW, proton beam of moderate intensity), the requirements on the detector are very stringent because it must be able to selectively and quickly acquire the relevant information related to each event. Innovative experimental techniques and detector technologies are thus required. An advantage of the REDTOP design is that the experimental apparatus can be exposed to beams of different particle species and different energies, thereby providing many opportunities to explore multiple aspects of fundamental processes. For example, the CP violating process $K^+ \to \pi^+\nu\bar{\nu}$ can be pursued with a stopped kaon beam generated from a 2–4 GeV proton beam. Also, a high intensity muon beam can be used to measure the proton radius. In all cases, the key issues are: (1) the sensitivity, resolution, and precision required for each physics process of interest, and (2) the ability of the experiment design and detector to meet the requirements.

VI.A. Detector Performance Studies

The primary source for the required sensitivity for any process comes from theory. With that in mind, extensive Monte Carlo (MC) simulations are done to test the performance of each component of the experimental apparatus and to estimate the ability to identify and/or reject backgrounds. At this time, a substantial set of computer codes has been assembled for REDTOP and extended to include both the design of the detector system as well as an expanded base of physical processes that can produce signals. Modifications continue to be made (*e.g.*, as noted above for the calorimeter). This proposal is intended to keep the process moving forward with a focus on the frontier physics that can be achieved.

Note: The current simulation codes are based on the ADRIANO calorimeter design [T1015-1, T1015-2, T1015-3]. As the R&D program discussed in Sec. IV.C proceeds, simulations will be made with the new ADRIANO2 design of the calorimeter.

Table II summarizes the four most important subsystems for REDTOP, the quantities to be measured, the items produced by the MC, and the status of event reconstruction analysis. Studies of triggering are being pursued by other groups in the Collaboration and will not be discussed here.

Sub-system	Measurements	Simulation	Reconstruction
O-TPC	Č ring param.; P_t	Hits	cheat pattern recog.
ADRIANO	S and Č *p.e.*	Hits + Digits	pattern recog. + dual-readout
Muon polarimeter	Scintillating light	Hits	–
Trigger	–	–	trigger module implemented

Table II. List of the experimental sub-systems and status of the simulation and reconstruction frameworks.

The overall signal/background ratio is critical to the sensitivity level of the experiment. It depends on all of the components and can be estimated from the pattern recognition and reconstruction in each sub-detector.

Among the four sub-systems to be studied, only the ADRIANO calorimeter has the full chain of simulation, pattern recognition, and reconstruction in place, since that technology has been consistently exploited by previous projects [4th-concept, T1015-1]. The codes will be expanded for the ADRIANO2 detector. On the other hand, simulation code for the OTPC and the Muon Polarimeter are more rudimentary and a good portion of the resources being requested with this EOI are intended to cover such deficiencies.

VI.B. Event Generation, Simulation, and Reconstruction Frameworks

Three software frameworks have been established for the physics and detector studies: *GenieHad* for the generation of primary events, *slic+lcsim*, and *ilcroot* for the event simulation, reconstruction and analysis. A brief description of them follows.

VI.B.1. GenieHad

The REDTOP *GenieHad* package [GenieHad] is an extension of the Genie framework [Genie] that is widely used in the neutrino community. It is used for simulating the primary interaction of the beam with the experimental apparatus. The extensions take into account non-neutrino interactions and more complex topological aspects needed in our case.

The core of *GenieHad* is a collection of interfaces to existing hadron interaction simulation packages that are being developed and maintained in the nuclear physics community. The underlying architecture takes care of the environment of the event (geometry of the apparatus, materials, beam profile and composition, targets, etc.), while the hadron interaction engine is called at run-time for each event in order to simulate the scattering at the nuclear level. With this approach the predictions from multiple nuclear interaction models can be compared to test the robustness and uncertainties of the simulations.

VI.B.2. slic+lcsim

The *Slic* [slic] and *lcsim* [lcsim] codes are, respectively, the simulation and reconstruction/analysis framework developed by the SID Collaboration [SID] for the ILC project, the Muon Collider project [MUX], and for the HPS experiment at JLAB [HPS]. A modified version of *slic* has been implemented by REDTOP [REDTOP-slic] in order to correctly handle the Čerenkov photons produced in the OTPC and in the dual-readout ADRIANO calorimeter. Similarly, a modified version of the geometry package of *lcsim* has been implemented in order to describe the particular layout of some

REDTOP subsystems. The framework has been shown to be very robust. The flexibility in the description of the detector geometry and of the detector response makes it ideal for the initial phase of REDTOP, where the design of each component is subject to frequent changes.

VI.B.3. ilcroot

The architecture of *ilcroot* is based on the ALICE offline system [Aliroot]. It has been initially developed for the MEG experiment at PSI, and then adopted by several projects and experiments (4th Concept, MUX, T1015, ORKA). The *ilcroot* framework uses a Virtual Monte Carlo interface (VMC) and is currently linked to the commonly used Geant3 and Geant4 codes that enables the user to build an application independent of the underlying Monte Carlo implementation. The concrete Monte Carlo is selected and loaded at run time. This kind of approach makes the VMC an ideal tool when switching from a fast to a full simulation, or when it is necessary to compare the predictions of different Monte Carlo systems, with the same detector geometry and data structure. The entire framework is based on the root CERN and on root I/O codes.

All three of these codes are fully functional and in use. Out of the several hadron interaction interfaces packaged in *GenieHad*, those corresponding to the Urqmd and to the Incl++ engines are being used in the current studies for REDTOP. Comparisons of the two nuclear models provides an extra level of confidence on the results. Currently, four different layouts for the REDTOP detector have been implemented in *slic*, while only one has been implemented in *ilcroot*. Both frameworks produce detector hits. The digitization of hits is included in the *lcsim* based simulation for all the sub-detectors of REDTOP while the ADRIANO calorimeter has a functional digitization module only in *ilcroot*. A full pattern recognition and reconstruction system is available only for the ADRIANO calorimeter. Similar functionalities to the OTPC are actively being developed. No reconstruction is currently available for the Muon Polarimeter. An identical situation is faced by *ilcroot*. A java module for implementing a Level-0 trigger is currently available only in *lcsim*. However, no algorithms have been implemented so far in that module. Table II summarizes the status of the REDTOP software.

VII. PRELIMINARY MONTE CARLO SIMULATIONS

This section summarizes some preliminary Monte Carlo studies that we have performed in order to understand the detector performance. Such studies will also guide us toward the optimization of the detector design.

VII.A. Detector Performance Studies

Currently, among the three detector technologies proposed for REDTOP, only the ADRIANO dual-readout calorimeter has received extensive R&D. For the OTPC, simulation and reconstruction algorithms are still being developed by the collaboration. This section summarizes the status of them.

VII.A.1. Performance of ADRIANO Calorimeter.

Because the design of an ADRIANO2 calorimeter depends on the results of on-going R&D, simulations for the calorimeter have been done only for the ADRIANO design. Most of the studies

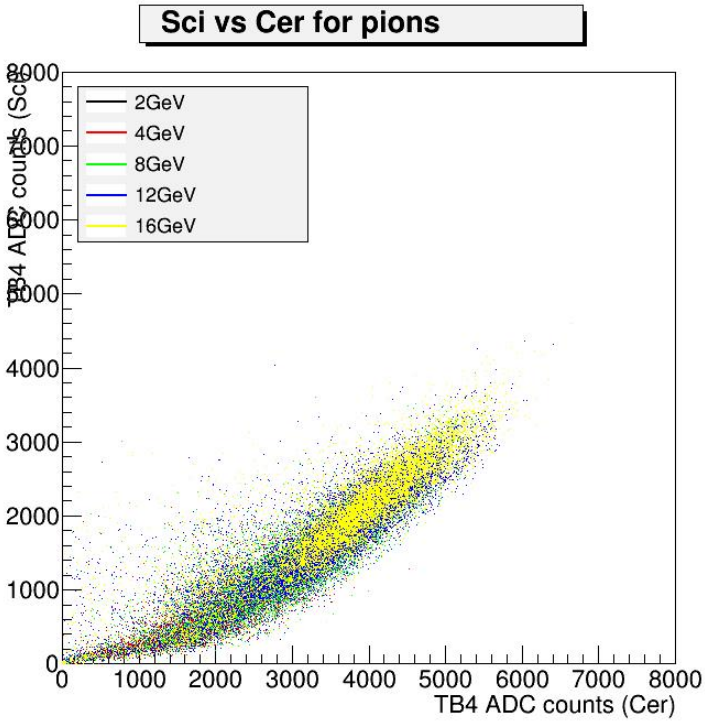

Figure 11. Scintillation vs. Čerenkov signals for ADRIANO prototype 2014-A with a pion beam of various energy (from a test beam at FTBF).

performed by the T1015 collaboration apply also to REDTOP because the proposed layout is identical to one of the prototypes built and tested. Fig. 11 shows typical signals obtained from a test beam of the ADRIANO 2014-A prototype, done at Fermilab in 2015.

Summing the Čerenkov (Č) and the scintillation (S) signals will provide the total energy of the particle. The compensation mechanism of dual-readout improves the hadronic energy resolution of the device, which is expected to vary from $\sim 20\%/\sqrt{E}$ up to $\sim 40\%/\sqrt{E}$, depending on the chosen layout (left plot in Fig. 12). On the other hand, due to the fully active volume of ADRIANO, the electromagnetic energy resolution is that of a typical lead glass calorimeter, namely $\sim 5\%/\sqrt{E}$, including instrumental effects (right plot in Fig. 12). By comparing the scintillation vs. the Čerenkov signals, one also has information about the ID of the particle that generated the shower (see Fig. 13).

VII.A.2. Performance of the OTPC

Four major effects are expected to contribute to the resolution of the OTPC: a) multiple scattering in the aerogel; b) non-uniformity of the refractive index of the Čerenkov radiators (aerogel and gas); c) electronics noise; and d) non-uniformity of the magnetic field. Because the latest techniques used to produce aerogels induce a non-uniformity in the latter smaller than 1%, while the gas performs even more uniformly, we neglect, for the moment, item b) as a source of measurement error. Similarly, the magnet we intend to use for REDTOP has been extensively tested by the Finuda Collaboration [Bert99] and shows an uniformity in the field better than 5% over the entire tracking volume. Consequently, our ongoing performance studies will take only a) and c) into consideration.

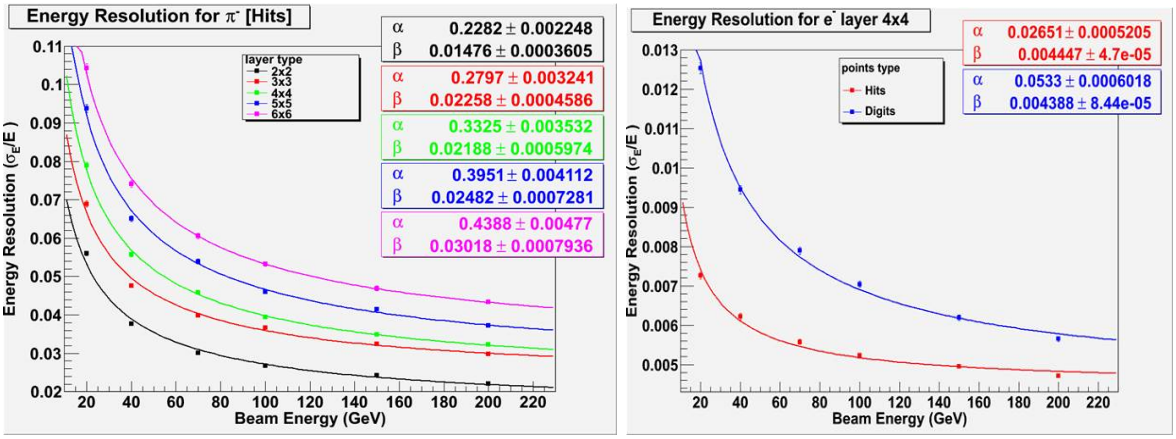

Figure 12. Hadronic (left plot) and electromagnetic energy resolution for various layout of an ADRIANO calorimeter (ilcroot simulations).

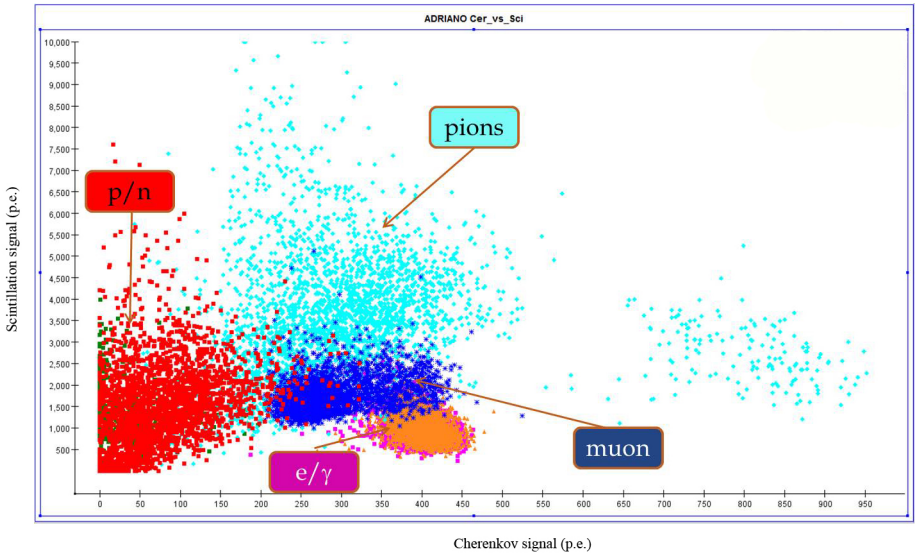

Figure 13. Plot of S vs. Č signals for 100-MeV particles in ADRIANO (ilcroot simulation).

The resolution on the Čerenkov angles affects the reconstruction of the momentum of muons and pions according to the formula

$$\frac{\delta\beta}{\beta} = \frac{\delta\theta_C}{\theta_C}, \tag{6}$$

while the effect of multiple scattering on the reconstruction of electrons (being reconstructed via their curvature in the magnetic field) is predominantly related to their directions.

The effect of electronic noise on the reconstruction of the ring is related to the presence of spurious hits which will degrade the fit to the Čerenkov angle. Such effect requires a dedicated study and it will be performed at a later stage of the proposal.

VII.A.3. Performance of the Active Muon Polarimeter

These studies are deferred to a later time, because there are plans to replace ADRIANO with ADRIANO2, whose improved granularity might render the Polarimeter no longer necessary.

VII.B. L0 Trigger Studies

The aim of this study is to devise a preliminary L0 trigger algorithm and to estimate the trigger efficiency for some of the physics processes and the amount of background rejected. Given the large rate of nuclear interactions expected between the proton beam and the target system, a fast L0 trigger is needed to reject most of the unwanted events. The two most rapid event signals are expected from the OTPC and the lead glass component of ADRIANO, both based on the prompt Čerenkov process. In this section, we will study the performance of a very crude L0 trigger obtained by counting the number of photo-sensors of the OTPC with hits and the total Čerenkov energy deposited in ADRIANO.

VII.B.1. Charged Event Trigger

A large majority of events of particular interest contains leptons in the final state. Those with charged pions in the final state are very abundant, and the trigger efficiency in these cases could be low without affecting the corresponding measurements. Fig. 14 shows a scatter plot of total hits in the OTPC vs. the integrated Č signal for three signal processes and background (top left: $\eta \to \gamma A'$ with M(A')=17 MeV; top right: $\eta \to \pi^+ \pi^- \pi^0$; bottom right: $\eta \to \gamma A'$ with $M(A') = 200$ MeV; bottom left: background). All events have been generated with the URQMD engine in GenieHad.

As one can immediately see from the plots, the background is mostly concentrated in the lower left corner of the plot. A cut on the two variables will yield a fraction of events shown in Fig. 15. The background has been simulated with the URQMD and the Incl++ engines of GenieHad. They produce similar results. Events with muons have a relatively lower efficiency, due to the particular choice of refractive indices of the aerogel used in the simulation.

VII.B.2. Neutral Events Trigger

A fewer number of events includes those with only photons in the final state. For such events, the information from the OTPC is not available and only the calorimeter can be used to reject background. A preliminary study has been conducted by using two discriminating variables: the total energy deposited in the lead glass of ADRIANO and the ratio of scintillation vs. Čherenkov energy.

Fig. 16 shows a scatter plot of $S/\check{C}$ vs. the integrated Č signal in ADRIANO for three signal process and background (bottom left: $\eta \to \gamma A'$ with $A' \to \gamma\gamma$; bottom right: $\eta \to H\pi^0$ with $H \to e^+e^-$; top right: $\eta \to 4\pi^0$; top right: background). All events have been generated by using the URQMD engine in *G*eneieHad.

A cut on the the two variables will yield a fraction of events shown in Fig. 17. The background has been simulated with the URQMD and the Incl++ engines of GenieHad. They produce slightly different results. As expected, the information from the ADRIANO calorimeter alone is inferior for rejecting the background.

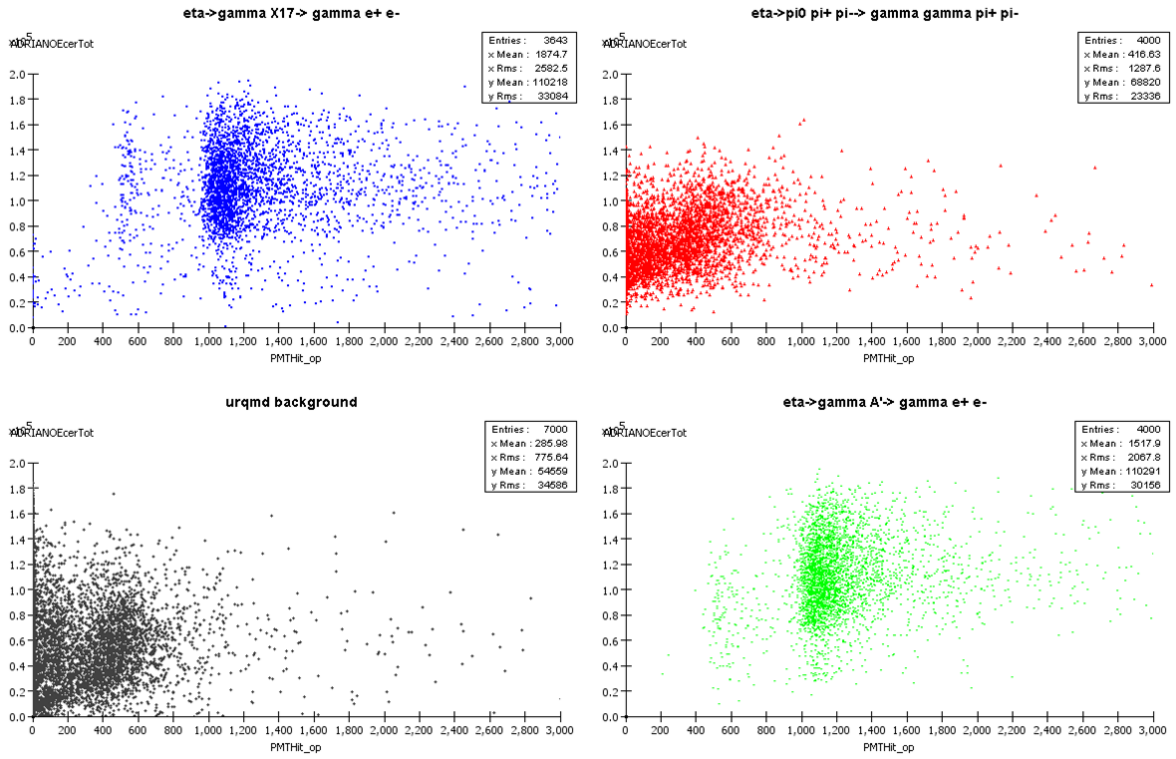

Figure 14. Plot of total hits in the OTPC vs. the integrated Č signal (GenieHad+Geant4 simulation). See text for a description of the plots.

Channels	Eff %
Urqmd bkg v4.1	1%
Incl++ bkg v3.1	1%
$p\ Be \rightarrow \eta \rightarrow \pi^{+}\pi\pi^{o}$	2%
$p\ Be \rightarrow \eta \rightarrow 4\pi^{o}$	2.9%
$p\ Be \rightarrow \eta \rightarrow e\,\mu$	75.6%
$p\ Be \rightarrow \eta \rightarrow A'\gamma \rightarrow e^{+}e^{-}\gamma$	88.3%
$p\ Be \rightarrow \eta \rightarrow X17\gamma \rightarrow e^{+}e^{-}\gamma$	81.8%
$p\ Be \rightarrow \eta \rightarrow e^{+}e^{-}\pi^{o}$	92.1%
$p\ Be \rightarrow \eta \rightarrow \mu^{+}\mu\pi^{o}$	21.9%

Figure 15. Fraction of events surviving the L0 trigger. See text for description.

VII.C. Further Trigger studies

We have made several studies related to the PID capability of a highly granular ADRIANO calorimeter (ADRIANO2). The fast direct readout of the glass could lead to a trigger design based on a local $S/\check{C}$ analysis of the cells that fire during the first few nanoseconds of the shower development. Most of the signal in that case corresponds to the EM component, which dominates the showers initiated

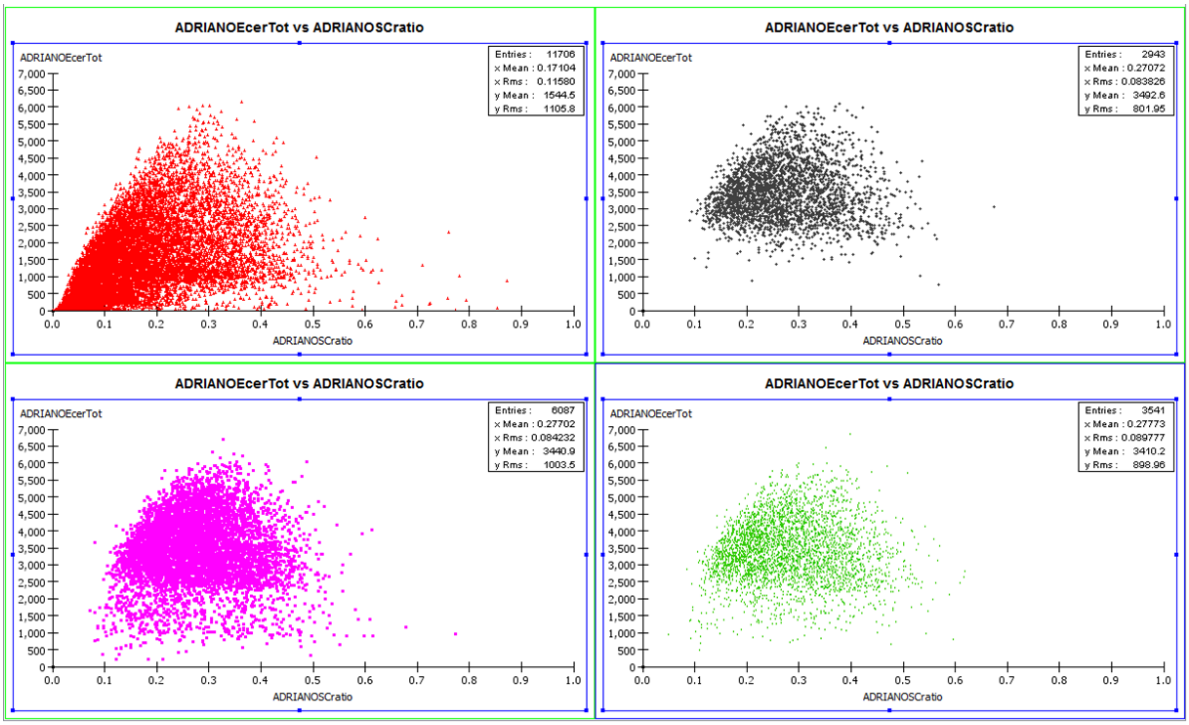

Figure 16. Plot of $S/\check{C}$ vs the integrated Č signal in ADRIANO (GenieHad+Geant4 simulation). See text for a description of the plots.

Channels	Eff %
Urqmd bkg v3.1	15.1%
Incl++ bkg v3.1	9.7%
Urqmd bkg v2.3	8.56%
$p\ Be \rightarrow \eta \rightarrow 4\pi^o$	84.9%
$p\ Be \rightarrow \eta \rightarrow e\ \mu$	50.8%
$p\ Be \rightarrow \eta \rightarrow A'\gamma \rightarrow e^+e^-\gamma$	80.8%
$p\ Be \rightarrow \eta \rightarrow A'\gamma \rightarrow \gamma\gamma\gamma$	80.4%
$p\ Be \rightarrow \eta \rightarrow e^+e^-\pi^o$	81.5%
$p\ Be \rightarrow \eta \rightarrow \mu^+\mu\pi^o$	34.8%

Figure 17. Fraction of events surviving the L0 trigger. See text for description.

by photons and electrons. Preliminary studies have indicated that excellent particle identification could be achieved for electrons.

Fig. 18 shows the efficiency and purity for electrons, as a function of their momentum, for the signal developed during the first 1 ns of the shower. The effect of such a trigger, as well as its extension to pions and muons, will be the subject of further studies.

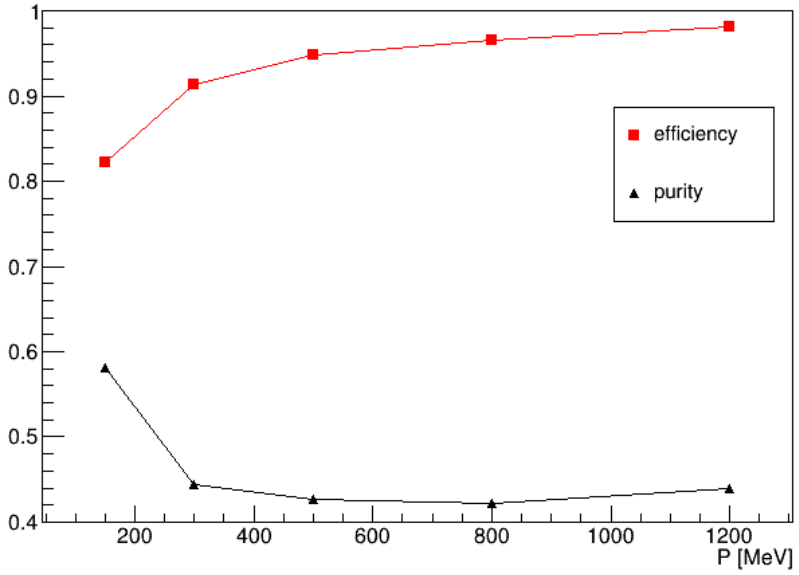

Figure 18. Plot of efficiency and purity for electrons based on a local $S/\check{C}$ analysis of the first 1 ns of the shower development.

VII.D. Physics Observables for the Golden Channels

The goal for these simulations is to understand the resolution of the physics observables for the three golden processes we have identified as well as to start an optimization procedure for the detector. For these studies, the detector resolution is simulated by an educated smearing of some parameters. The latter are varied within a reasonable range and the effect on the observable is recorded. The detector parameters used are the following:

- The energy resolution in the calorimeter is parameterized as

$$\frac{\sigma_E}{E} = \frac{\alpha}{\sqrt{E}} \oplus \beta. \tag{7}$$

- We conservatively assume that a photon impinges on the calorimeter at the center of a cell. No attempt has yet been made to improve the estimate of this parameter with a full reconstruction of the shower shape.

- Because no reconstruction algorithms of a track in the OTPC exist at this time, we assume that the dominant effects on the momenta and directions of charged tracks in the OTPC reconstruction is due to the multiple scattering of the particles in the aerogel. For electrons, we add in quadrature the effects due to all the matter in the OTPC (gas + aerogel) and the finite size of the photosensors.

Preliminary results for the Golden Channels are discussed in the following subsections.

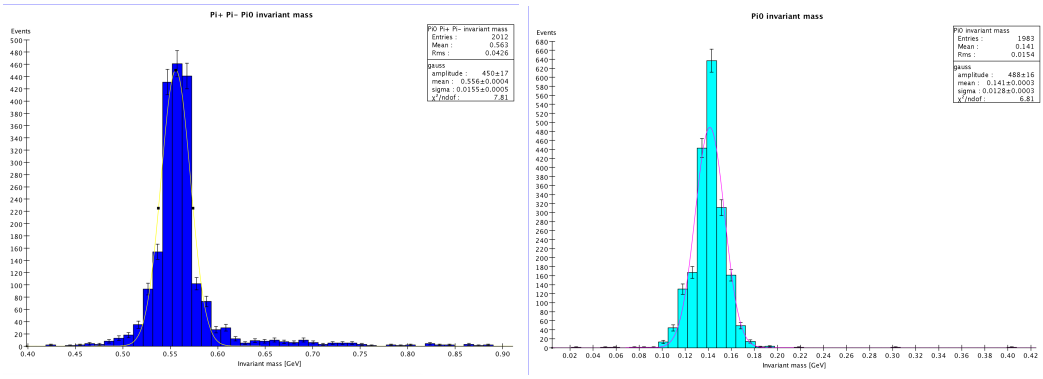

Figure 19. Plot of η (left) and π^0 invariant masses in $\eta \to \pi^+\pi^-\pi^0$ (GenieHad+Geant4 simulation). The baseline OTPC + ADRIANO2 is assumed for REDTOP.

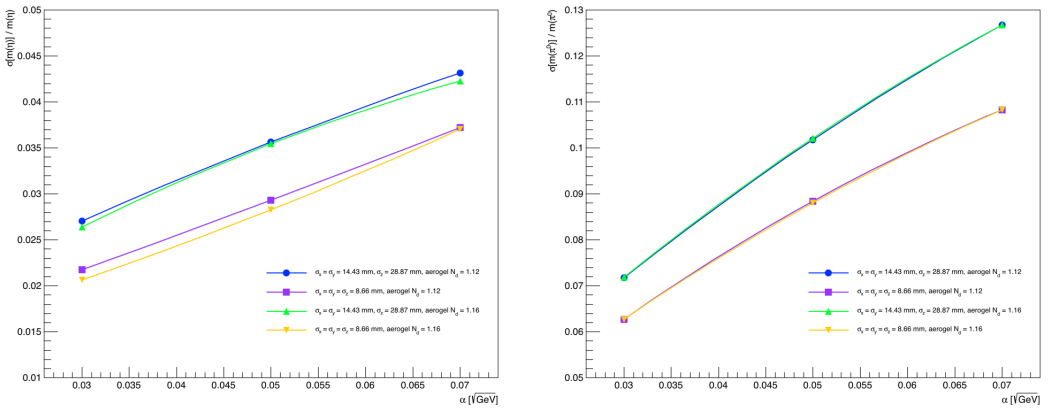

Figure 20. Plot of changes in η (left) and π^0 (right) invariant masses in $\eta \to \pi^+\pi^-\pi^0$ vs. the energy resolution of the calorimeter.

VII.D.1. $\eta \to \pi^+\pi^-\pi^0$ Dalitz Asymmetries

The observables for this process are the invariant mass of the two photons, the invariant mass of the three reconstructed pions, and the asymmetry of the Dalitz plot. Typical distributions for the expected invariant masses of the η and π^0 mesons, corresponding to a baseline OTPC and a granular version of ADRIANO (ADRIANO2), are shown in Fig. 19.

Fig. 20 summarizes the dependence of the invariant masses of the η and π^0 mesons on the energy resolution parameter α in Eq. 7 of the calorimeter. The curves represent different choices of estimated standard deviations of other calorimeter and aerogel properties. Similarly, Fig. 21 shows dependencies with respect to position resolution σ_x of the calorimeter.

Changes in the detector layout within reasonable ranges induce only moderate changes in the resolution of the reconstructed masses. Changes of the order 30% in the density of the aerogel do not affect the invariant masses to any appreciable extent. Thus, for this decay channel, the dominant effect on the mass reconstruction is related to the performance of the calorimeter.

Preliminary studies of the Dalitz plot of the three pions along with those of the X component of the asymmetry (cf. Eq. 1), based on about 10^5 simulated events and for a large range of detector parameters, indicate that a sensitivity comparable to that of the KLOE experiment [KLOE-CP])

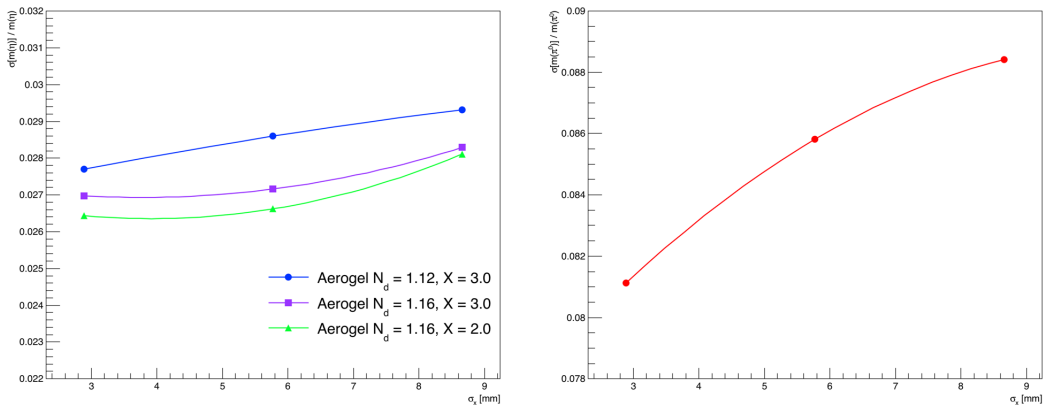

Figure 21. Plot of changes in η (left) and π^0 (right) invariant masses in $\eta \to \pi^+\pi^-\pi^0$ vs. the position resolution of the calorimeter.

can be obtained. Scaling by the total yield of η mesons and the reconstruction efficiency, we expect the statistical error on the asymmetry to be improved by about one order of magnitude.

VII.D.2. $\eta \to \gamma A'$ with $A' \to e^+e^-$

The signature of dark photons in meson decays is a peak in the invariant mass spectrum at $m_{ee} = m_{A'}$. The success of such a search will depend crucially on a good invariant mass resolution for the lepton pairs. If the mixing parameter of dark photons is below 10^{-5}, its signature will be not only a mass peak, but also a displacement of the A' creation and decay points.

Plots similar to those of the previous subsection are being studied. The invariant mass resolution of the A' from the simulations is about 2.5%. Again, changes in the detector layout within reasonable parameter ranges induce only moderate changes in the resolution of the reconstructed masses. Changes of the order 30% in the density of the aerogel do not affect the invariant masses to any appreciable extent. Thus, the dominant effect on the mass reconstruction for this decay mode, is related to the performance of the calorimeter.

VII.D.3. $\eta \to \pi^0 H$ with $H \to \mu^+\mu^-$

A light Higgs-like scalar can couple to the light quarks with a strength proportional to a Yukawa coupling. For the case of the two-Higgs doublet model, the coupling of light scalars to down or strange quarks can be enhanced without violating flavor constraints. The signature of such a light scalar would be an enhancement of $\eta \to \pi^0\mu^+\mu^-$ rate compared to a very suppressed two-photon mediated Standard Model rate. Moreover, the invariant mass of the lepton pair should reconstruct to m_H.

As with the previous two decay modes, changes in the detector layout within reasonable ranges induce only moderate changes in the resolution of the reconstructed masses. The invariant mass resolution of the H from the muons in the simulations is about 1%, independent of the calorimeter position resolutionm σ_x.

Changes of the order 30% in the density of the aerogel affect the invariant mass of the reconstructed H scalar considerably. However, even in the worse case, the resolution is still of the order of 1%.

VII.E. Summary of Preliminary Monte Carlo Simulations

The studies presented in this section are primarily meant to test the simulation machinery and to establish the base for the simulation work needed for the development of a full proposal. Nonetheless, the studies performed have already given important indications that will guide us to a re-design of the detector in order to improve the sensitivity to the rare processes. Here is a summary of such indications.

- Background rejection. An analysis of the $\sim 1\%$ background events that survive the simple L0 trigger described above shows that the vast majority of such events correspond to photons from the decay of neutral pions converting in the beam pipe and the aerogel. Because the latter amounts to several percent of the radiation length, the probability of triggering a non-η event is on the order of 50%. A clean way to strongly reduce such background is by adding a tracker upstream of the aerogel so as to disentangle genuine electrons that originate from the primary vertex from electron-positron pairs that originate in the aerogel. Fiber trackers with minimal material (a few percent of $X0$) have been designed for the upgrade of the LHCb experiment and are currently in production.

- Several processes within the scope of REDTOP correspond to a bump search of the invariant mass of reconstructed particles. In order to identify such accumulations of events from an expected large continuous background, the mass resolution of combined particles needs to be improved. A more detailed analysis of the spread indicated that the dominant factor in the invariant mass resolution is due to a poor reconstruction of the impinging point of a photon in the calorimeter. The longitudinal layout of ADRIANO, where the z-coordinate is reconstructed with light division or time difference techniques, is sub-optimal for this task. Consequently, a more finely segmented calorimeter is highly desirable. It could also render the Muon Polarimeter superfluous if the full chain of the muon decay is reconstructed (for example, with Particle Flow Analysis (PFA) techniques [PFA-2009]).

- Because the η production cross section is about two orders of magnitude smaller than the full inelastic cross section of the protons on the Be target, a L0 trigger needs to reject at least four orders of magnitude of that background. In addition to the addition of the fiber tracker (as discussed above), two factors would help with achieving the desired rejection rate: (a) fast timing (~ 50 ps resolution) in the calorimeter and (b) granularity sufficient to perform a PFA of the shower at the L0 trigger level.

A new detector layout is being designed based on the above indications. A new fiber tracker with the same technology as that adopted by LHCb (LHCb-PUB-2015-008) will yield a position reconstruction resolution of the order of 80 μm, with a material budget of about 1% X/X_0 per layer and a single hit efficiency of 99%. The ADRIANO calorimeter will be upgraded to a new, ADRIANO2 version, where some of the scintillating and lead glass strips will be replaced by tiles with direct readout through SiPMs optically coupled to the latter. The upgrade will provide a calorimeter with fast timing resolution ($<$50 ps) due to the direct light capture technique, with no scintillating processes slowing the formation of the signal, and excellent granularity. Due to the fine granularity, PFA tools can be applied to the whole event, allowing for precision measurements, and further enhancing the particle identification (PID) capability of the dual-readout technique. The precision timing of EM showers will allow events from multiple interactions (pile-up) to be disentangled. The Dual-readout discriminating technique could be applied at the L0 trigger for fast reduction of unwanted events.

VIII. STATUS AND PLANS

During the past two years, we have initiated the formation of a formal REDTOP collaboration, with the goal of generating a much more complete Letter-of-Intent within about one year and, subsequently, a full proposal within, at most, two years.

Our most immediate plan is to re-design the detector according to the results of our preliminary simulations. Several layers of a thin fiber tracker and the upgrade of the calorimeter to an ADRIANO2 design will be implemented in the detector layout as indicated in Sec. VII.E

Implementation of the new detectors in the simulations will take a few months, while the studies leading to a full LOI will take the rest of the year. The two software frameworks implemented for such studies, *i*lcroot and *s*lic+lcsim, are solid and able to accommodate all steps needed for the studies, which include event generation, Geant4 transport through the detector matter, and digitization of the detectors. Pattern recognition and event reconstruction in the OTPC and in ADRIANO2 will probably take more than one year with the support of experienced scientists.

The design of the accelerator complex is in its early stages. Although the preliminary studies have indicated that there are no show-stoppers in the conceptual design, we would like to complete a full design within two years. Continuous support from Fermilab's AD is of paramount importance for achieving that goal.

Preliminary engineering studies have demonstrated that the REDTOP detector could be accommodated in the AP50 hall. However, the tight space and the limitation of available tools require a careful design of the detector component and of the installation procedure. We foresee a more adequate involvement of Fermilab Engineering Dept. even in this early stage of the project, in order to avoid potential design flows that could be costly to fix at a later stage of the experiment.

Our long term plans are fully constrained by the next Snowmass/P5 process, in which REDTOP intends to participate. In that framework, REDTOP detector would not be able to start constructions before about 2021-2022. However, given the novelty of the detector technologies proposed, we foresee at least two, and possibly three, years of detector R&D, whose support could be initiated already in 2018 upon a favorable recommendation by Fermilab's PAC.

IX. CONCLUSIONS

The goals of REDTOP are to push the sensitivity limits of core conservation laws by many orders of magnitude, as well as other processes that can open the doorways to Physics Beyond the Standard Model. The experiment will bring new and innovative detector methodologies to the task, including an ADRIANO2 calorimeter for which R&D funding is being sought from DOE. The new technologies will be available to and enrich future HEP experiments. The continued development of the experiment by the Collaboration, assuming no show-stoppers, will need the endorsement and support of Fermilab.

The collaboration currently consists of scientists and engineers from Fermilab, other laboratories, and universities. New collaborators are being actively recruited. Work is actively underway on the design of the beam line and detector components. Extensive computer simulations are planned.

Cost and resource estimates are in their very early stages and will be under close scrutiny in the next several months. REDTOP is proposing to re-use some of the facilities available at Fermilab, in particular, the existing AP50 Experimental Hall. Possible reuse of existing solenoids (for example,

from the Finuda experiment) is being pursued. A considerable amount of money would be saved, and we anticipate that most of the cost of the project will be related to the R&D for the detectors and on the construction of the experimental apparatus.

In addition to being able to push the realm of new physics to better sensitivities, REDTOP will provide an abundance of opportunities for students to pursue theses, including work involving physics, beams, and detectors of new capabilities. The ability to serve as an "η/η'-factory" by having multiple runs at different energies, along with pursuing fundamental issues in physics will enrich the community for many years.

Appendix A: Full List of REDTOP Decay Channels

Appendix B: Detailed Flux Analysis

A detailed calculation of the particle fluxes through the REDTOP detector has been performed with the latest version of MARS15 [MARS15]. The areas most sensitive to large radiation are the external walls of the OTPC and the regions near the beam pipe. In the former case, photo-sensors are used to detect single photo-electrons generated by the Čerenkov radiators. Such sensors are usually very sensitive to radiation as their Dark Count Rate (DCR) increases rapidly with the accumulated dose. In the latter case, the plastics in the core of scintillating fibers are degraded and the light yield is diminished.

Two quantities: "*1-MeV equivalent neutron fluency*" and the integrated dose are plotted for the forward endplate (Fig. 22) and the barrel (Fig. 23) of the OTPC, and for the area around the beam pipe being occupied by a fiber tracker (Fig. 24).

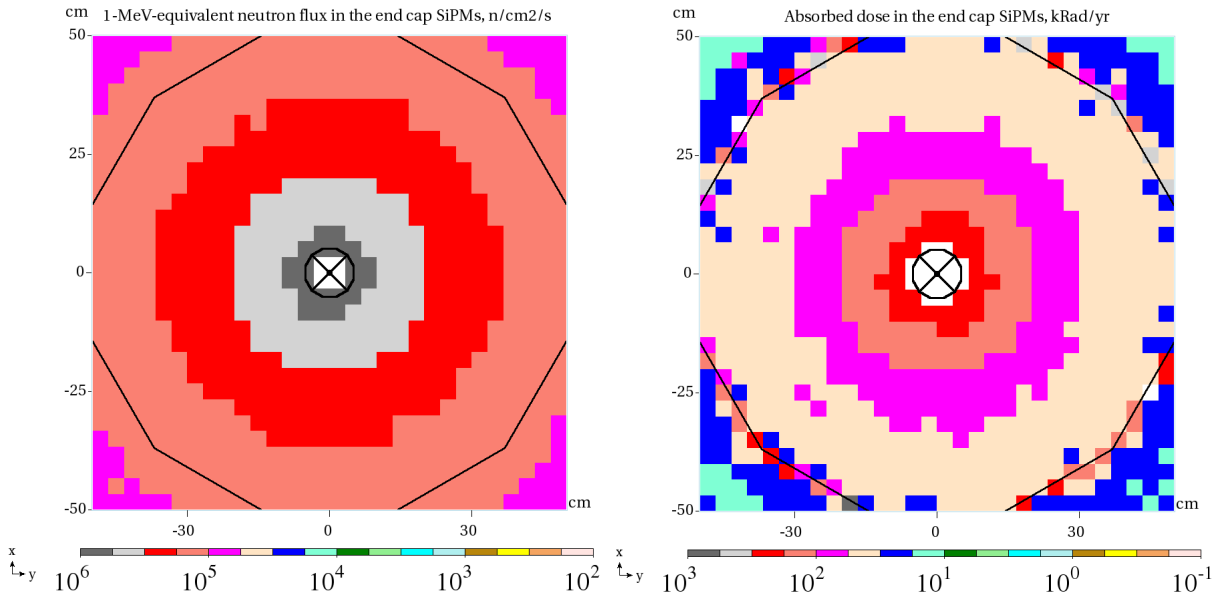

Figure 22. "*1-MeV equivalent neutron fluency*" flux (left) and absorbed dose expected in the OTPC forward endplate for a 30 W proton beam.

The studies presented here are preliminary and indicate that the radiation in the detector area is relevant and that the radiation damaged needs to be closely monitored. Furthermore, while the absorbed dose in the barrel is about one order of magnitude smaller than in the forward endcap, the NEQF is only about 5-6 times smaller, indicating that about half the flux of particles particles irradiating the photo-sensors are not neutrons, Further investigation on the matter is required.

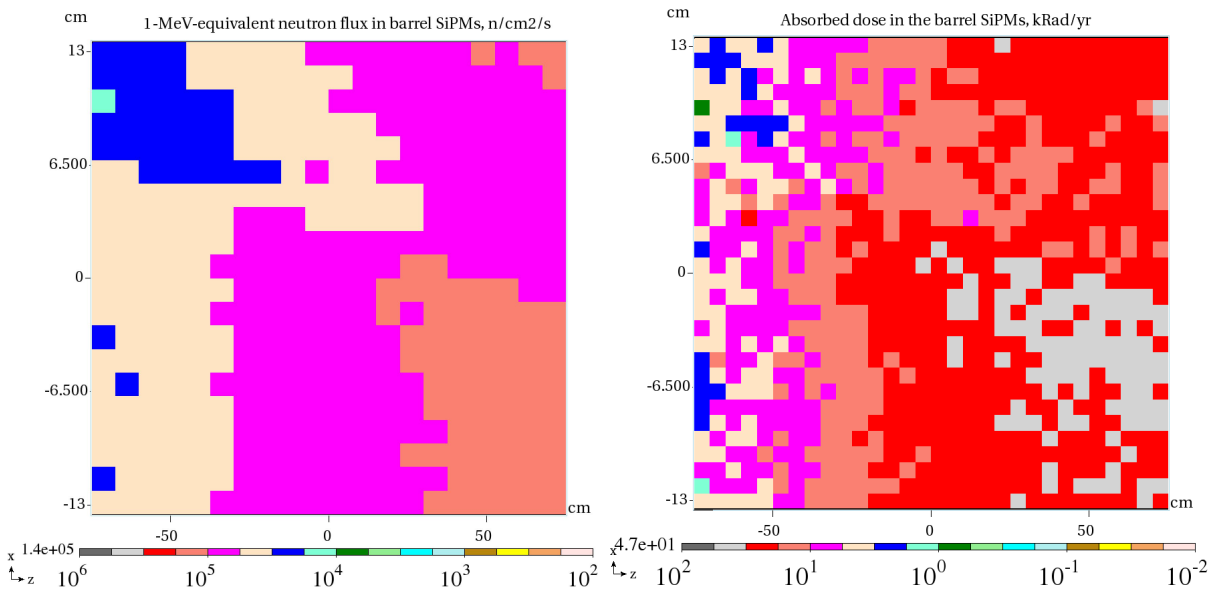

Figure 23. "*1-MeV equivalent neutron fluency*" flux (left) and absorbed dose expected in the OTPC barrel for a 30-W proton beam.

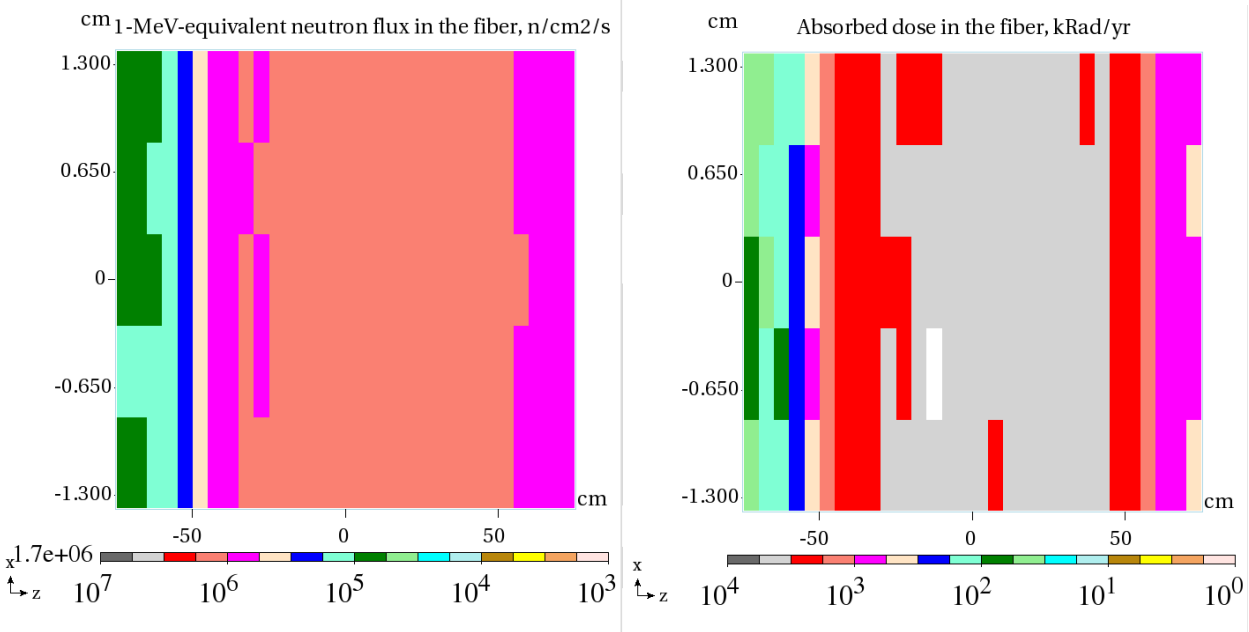

Figure 24. "*1-MeV equivalent neutron fluency*" flux (left) and absorbed dose expected in the OTPC fiber tracker for a 30-W proton beam.

Appendix C: Data Rates

In this section we discuss some of the arguments we used to estimate the data rates quoted in the Sec. V and summarized in Table I. Please be aware that these estimates are still rather crude and are meant to be not much more significant than orders of magnitude. More refined studies are needed to progress towards a full design of the REDTOP trigger.

C.1. Data Rates from the Detector

We do not anticipate having an independent path for the data used by the trigger. All data from all detector components are digitized continuously in real time and transmitted to the subsequent trigger levels whose task is to remove unwanted events. Data can also be and/or reformatted in the process. We assume that the chain of subsequent trigger-level stages will be operated as a dead-timeless pipeline and that sufficient local storage will be provided at each stage to allow the formation of data queues so that statistical fluctuations will be smoothed out and only the average data rates will be relevant, at least to first order.

We consider four different sub-detectors: the OTPC, the Čerenkov light and the scintillation light sections of the calorimeter, and the fiber tracker. The amounts of data generated by each sub-detector are estimated in the following subsections and summarized in Table III. The resulting total is 9,880 bits which we round up to 10 *kb*.

C.1.a. The OTPC

The histogram in Fig. 25, obtained from Monte Carlo simulation, shows the distribution of the number of channels in the OTPC hit by at least one optical photon, per inelastic collision. The average is 86.22 which we round up to 100. We assume that, after zero suppression, each hit will be encoded with a channel number (18 bits), pulse height (8 bits) and timing (8 bits), for a total of 34 bits. Therefore, the total number of bits to be transmitted from the OTPC, for each inelastic collision, is $100 \times 34 = 3400$.

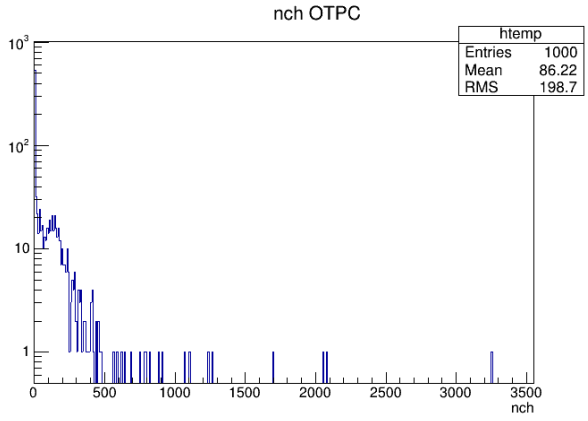

Figure 25. Number of OTPC channels fired per inelastic collision.

C.1.b. Calorimeter: Čerenkov Light

The histogram in Fig. 26 shows the distribution of the number of Čerenkov light channels in the ADRIANO calorimeter with non-zero energy deposit. The average is 23.28 which we round up to 30. We assume that, after zero suppression and waveform analysis, each hit will be encoded with a channel number (16 bits), pulse height (16 bits) and timing (8 bits), for a total of 38 bits. Therefore, the total number of bits to be transmitted from the Čerenkov section of ADRIANO, for each inelastic collision, is $30 \times 38 = 1140$

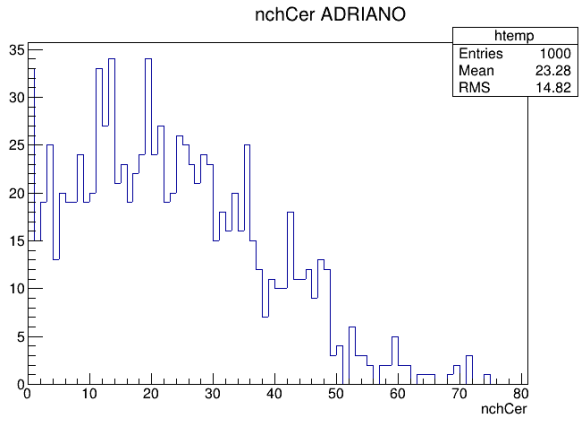

Figure 26. Number of ADRIANO Čerenkov channels fired per inelastic collision.

C.1.c. Calorimeter: Scintillation Light

The histogram in Fig. 27, obtained from Monte Carlo simulation, shows the distribution of the number of scintillation light channels in the ADRIANO calorimeter with non-zero energy deposit, for each inelastic collision. The average is 29.58 which we round up to 30. We assume that, after zero suppression and waveform analysis, each hit will be encoded with a channel number (16 bits), four waveform parameters (32 bits each) timing (8 bits), for a total of 152 bits. Therefore, the total number of bits to be transmitted from the Čerenkov section of ADRIANO, for each inelastic collision, is $30 \times 152 = 4560$.

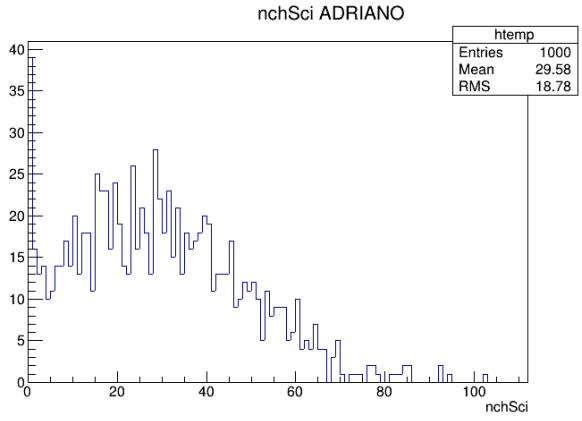

Figure 27. Number of ADRIANO scintillation channels fired per inelastic collision.

C.1.d. Fiber Tracker

The fiber tracker is composed of 6 layers of $250\mu m$ scintillator fibers arranged on a cylinder of 5 cm radius. The total number of fibers is about 7,500 and 13 bits are needed to encode their individual address. Zero suppression in the front end produces a list of addresses of fibers which contain a non zero deposited energy. An average of ten charged particles are expected to traverse the fiber tracker for each inelastic collision, hitting an average of six fibers each (one per layer). The average total number of bits needed to encode the fiber tracker hit list is, therefore $6 \times 10 \times 13 = 780$.

C.2. Data Rates After Level 0

The Level 0 trigger selection is based on thresholds on the number of channels hit in the OTPC and on the amount of energy deposited in the Čherenkov section of the ADRIANO calorimeter. It reduces the event rate by about a factor 100 but, as a consequence of the selection requirements, the average occupancy of events passing Level 0 is higher than those failing it. This means that the amount of information that needs to be transmitted, on average, per event out of Level 0 is going to be higher than on input. The increase of information per event caused by the Level 0 selection has been estimated by simulation and has resulted in an increase of a factor 8.5 for the OTPC and a factor 2.1 for the calorimeter. By applying these factors to numbers in Table III we obtain a total event size of 50 *kb* at the output of Level 0.

C.3. Data Rates to Permanent Storage

The Level 2 processor farm performs a complete reconstruction of each event filtered by Level 1. The information generated by the reconstruction (particle momentums, species, charge, vertices, etc., together with additional relevant parameters like goodness of fits etc.) is added to the "raw" data before permanent storage. We tentatively assume the increase in stored information to be a factor of 2 and estimate 100 kb for the final event size.

sub-detector	*data volume bits*
OTPC	3,400
Čerenkov	1,140
Scintillation	4560
Fiber tracker	780
Total	9,880

Table III. Data volumes per inelastic collision for different sub-detectors

Appendix D: Support

The REDTOP Collaboration includes groups from Universities and Laboratories around the world, enticed by the broad physics program that can be achieved and by the relatively short overall duration, which fits nicely with the schedule of a typical Ph.D. thesis in HEP. Because the collaboration has been forming with little or no pre-existing support, REDTOP is severely limited by its current level of resources. This situation is exacerbated by the novelty of the experimental techniques that require development of entirely new simulation and reconstruction algorithms.

Currently, the main support is from Fermilab's Accelerator Division for an initial beam design and for a preliminary understanding of radiation flowing into the detector components (for aging consideration and optimization of radiation damage studies). Some students have been available to help with physics and detector studies. Many collaborators are contributing beyond their regular jobs, as they genuinely believe in the project.

Some of the U.S. Universities participating in REDTOP have recently responded to a solicitation from DOE, requesting support for R&D on the ADRIANO2 calorimeter and for physics and detector studies necessary for a full proposal. No information is available at this time on the status of the proposal.

In such a scenario, a minimal level of support from Fermilab, for a two-year time period would considerably improve the ability to optimize the design of the detector. A well thought-out detector design would enhance the physics reach of the experiment. Such support could span over several possible areas:

D.1. Accelerator design and radiation studies.

It is important that the current support for designing the accelerator and for assessing the radiation fluxes throughout the detector be maintained, and possibly increased. Although the preliminary studies have indicated that there are no show-stoppers in the current deceleration and extraction strategy, we are still far from a comprehensive design. Furthermore, future changes in the detector layout and in the related electronics will require updated assessments of the radiation doses absorbed.

D.2. Mechanical engineering.

The AP50 enclosure where REDTOP would be installed presents severe challenges. Specifically, the space for the assembly is quite limited and connected to a hatch through a relatively narrow pathway. Also, the ceiling of AP50 prevents the installation of a cryogenic valve box without a modification of either the hall or of the whole cryogenic supply systems. In addition, the only available crane in the area has a lift limit of only two tons, and no space to refurbish it with a larger one.

These issues will considerably impact the design of the detector. It is important to have a good understanding of the size and impact of each issue, including assembly procedures and the fixtures and jigs required, before the detector layout is finalized and simulations for the final proposal are launched. The total engineering effort required to complete the above tasks has been estimated at about 3.5 FTE for Engineers (of which, 1.5 FTE is for a cryogenic engineer) plus 1 FTE for a drafter. Some of the engineering and drafting tasks could be absorbed by the collaborating institutions. However, a Fermilab mechanical engineer is necessary for some tasks, amounting to about 1 FTE.

D.3. Trigger.

We believe that the trigger is the most important component of a High Intensity experiment such as REDTOP. The data rate requirements for the online systems mean that a trigger must be capable of recognizing the Čerenkov rings in the OTPC even at the Level 0. Such a feature has never been implemented in a HEP experiment. Advanced knowledge of novel and fast trigger techniques exist at Fermilab, and none of the collaborating groups could possibly match it. Some support to design the trigger and to coordinate the effort with the external collaborators would be extremely valuable for the preparation of a successful proposal.

D.4. Physics and detector studies.

Finally, considering the excellent expertise available at Fermilab for simulations of HEP experiments, we would very much benefit from some help with detector and with physics studies, to a level not exceeding 0.6 FTE.

A summary of the support requested for a two-year period is summarized in table

Table IV. Support requested for REDTOP proposal

Task	FTE
Accelerator design and radiation studies	0.5
Mechanical engineering	1.0
Mechanical drafter	0.5
Trigger design	0.2
Physics studies	0.3
Detector performance studies	0.3

Acknowledgments

We wish to thank Fermilab's Accelerator Division for its support to the project and for providing the resources needed for the simulations of the accelerator and for assisting with the computing related to the physics and detector studies.

[4th-concept] http://www.linearcollider.org/ILC/physics-detectors/Detectors/Detector-LOIs
[Adlarson] P. Adlarson *et al.*, Phys. Rev. C **90**, 045207 (2014).
[Aliroot] http://aliweb.cern.ch/offline/
[Amb08] F. Ambrosino *et al.*, JHEP **0805** 006 (2008).
[Amb09] F. Ambrosino *et al.*, Phys. Letters **B675**, 283 (2009).
[Bert99] M. Bertani *et al.*, Nuclear Physics B (Proc. Suppl.) **78** 553 (1999).
[G-2] J. Miller, E. de Rafael, and B. L. Roberts, Rept. Prog. Phys. **70**, 795 (2007).
[Feng16] J. Feng *et al.*, https://arxiv.org/pdf/1604.07411v1.
[Gard04] S. Gardner and J. Tandean, Phys. Rev. D **69**, 034011 (2004).
[Genie] http://www.genie-mc.org/
[GenieHad] http://redtop.fnal.gov/the-geniehadevent-generation-framework/
[HPS] M. Battaglieri *et al.*, Nuclear Inst. and Methods in Physics Research, A **777**, 91 (2015).
[Johnstone] J. Johnstone and M.J. Syphers, arXiv:1612.07777 [physics.acc-ph] FERMILAB-CONF-16-509-APC (2016).
[Joram15] C. Joram *et al.*, JINST **10** C08005 (2015).
[JS02] C. Jarlskog and E. Shabalin, Physica Scripta **T99**, 23 (2002).
[KLOE-CP] A. Anastasi, D. Babusci, *et al.*, J. High Energ. Phys. **1605** 019 (2016).
[Lay72] J. G. Layter, Phys. Rev. Lett. **29**, 316 (1972).
[lcsim] https://confluence.slac.stanford.edu/display/ilc/LCSim+Tutorials
[MARS15] N.V. Mokhov and C.C. James, The MARS Code System User's Guide, version 15(2016), https://mars.fnal.gov/
N.V. Mokhov et al., MARS15 code developments driven by the intensity frontier needs, Prog. Nucl. Sci. Technol., **4**, 496 (2014)..
[MSP16] Pere Masjuan and Pablo Sanchez-Puertas, J. High Energ. Phys. **1608** 108 (2016).
[MUX] http://map.fnal.gov/
[Nef94] B. M. K. Nefkens in *Proceedings of the International Conference on Mesons and Nuclei at Intermediate Energies*, Ed. by M. K. Khankhasayev and Zh. B. Kurmanov, (World Scientific, Singapore, 1995).
[NgP92] J. N. Ng and D. J. Peters, Phys. Rev. D **46**, 5034 (1992).
[NgP93] J. N. Ng and D. J. Peters, Phys. Rev. D **47**, 4939 (1993).
[ORKA] `https://www.fnal.gov/directorate/program_planning/Dec2011PACPublic/ORKA_Proposal.pdf`
[PADME] M. Raggi *et al.*, http://arxiv.org/pdf/1501.01867.pdf
[PDG] Particle Data Group, Chinese Phy. C **38**, No. 9 (2014).
[Pet10] Thimo Petri, *Anomalous decays of pseudoscalar mesons*, Diploma Thesis, Institut fr Kernphysik Forschungszentrum Julich, 2010 (arXiv:1010.2378).
[PFA-2009] M. A. Thomson, Nucl. Instrum. Meth. **A611**, 25 (2009).
[Pospelov08] M. Pospelov and A. Ritz, arxiv.org/pdf/0810.1502.pdf
[Prak00] S. Prakhov *et al.*, Phys. Rev. Lett. **84**, 4802 (2000).
[REDTOP-slic] http://redtop.fnal.gov/the-slic-simulation-framework/
[SID] http://pages.uoregon.edu/silicondetector/
[slic] https://confluence.slac.stanford.edu/display/ilc/SLIC
[T1015-1] C. Gatto *et al.*, J. Phys.: Conf. Ser. **587** 012060 (2015).
[T1015-2] C. Gatto *et al.*, J. Phys.: Conf. Ser. **404** 012030 (2015).
[T1015-3] C. Gatto *et al.*, *Talk presented at the International Workshop on Future Linear Colliders* (LCWS15), Whistler, Canada, 2-6 November 2015.
[T1059] Henry Frisch, Technical Scope of Work for OTPC, `https://web.fnal.gov/experiment/FTBF/TSW\%20Library/T1059\_tsw.pdf`; see also E. Oberta and H. J. Frisch, http://arxiv.org/abs/1510.00947.
[WASA14] P. Adlarson *et al.*, Phys. Rev. C **90**, 045207 (2014).